Acknowledgement

First of all, I would like to express my deepest gratitude to my supervisor, professor Ursula Sonnewald, for all the support, guidance and positive feedback that I have received since I first started with the thesis. This has both helped and motivated me, and I strongly believe I could not have had a better supervisor. The same goes for Mussie Ghezu, the Ph.D. student who has patiently spent a lot of his time teaching and helping me when he probably had more important things to do. አመሰግናለሁ! Additionally, I would like to thank Lars Evje, who has also been extremely patient and helpful in the lab, as well as during the write-up of the thesis. To Tesfaye Terfera, a fellow master student, who has kept me with great company in the office. A big አመሰግናለሁ to you too! I also want to thank the rest of the group for the good working atmosphere they provide. I have thoroughly enjoyed being part of it.

Other people I would like to thank include Anne Seim Fuglset, a fellow master student, who has become one of my closest friends since we started the degree in 2011. I have really valued our daily contact, and you have been a tremendous support and provided lots of great entertainment since then! In addition to this, my housemates, family and other friends have also been highly supportive and deserve a big reward (in theory).

Abbreviations

CNS - central nervous system
CSF - cerebral spinal fluid
BBB - blood-brain barrier
AP - action potential
iGluR - ionotropic glutamate receptor
mGluR - metabotropic glutamate receptor
GABA - γ-aminobutyric acid
GFAP - glial fibrillary acid protein
AQP4 - aquaporin 4
GS - glutamine synthetase
GLUT - glucose transporter
ATP/ADP/AMP - adenosine tri-/di-/monophosphate
TCA - tricarboxylic acid
Glc-6-P - glucose-6-phosphate
Acetyl-CoA - acetyl coenzyme A
PDH - pyruvate dehydrogenase
OAA - oxaloacetate
PC - pyruvate carboxylase
$NAD(P)^+$ - nicotinamide adenine dinucleotide (phosphate), oxidised form
NAD(P)H - nicotinamide adenine dinucleotide (phosphate), reduced form
$FADH_2$ - flavin adenine dinucleotide
GDH - glutamate dehydrogenase
PAG - phosphate-activated glutaminase
GAD - glutamate decarboxylase
MCT - monocarboxylic acid transporter
TLE - temporal lobe epilepsy
MTLE - mesial temporal lobe epilepsy
LTLE - lateral temporal lobe epilepsy
IPI - initial precipitating injury
SE - status epilepticus
AED - antiepileptic drug
EEG - electroencephalogram
CAE - childhood absence epilepsy
JAE - juvenile absence epilepsy
JME - juvenile myoclonic epilepsy
MAE - myoclonic absence epilepsy
KA - kainic acid
GAERS - Genetic Absence Epilepsy Rats from Strasbourg
NMDA - *N*-Methyl-$_D$-aspartate
CRS - carisbamate, S-2-O-carbamoyl-1-O-chlorophenyl-ethanol
SWD - spike-and-wave
NDA - new drug application
MAA - medical authorization application
NMRS - nuclear magnetic resonance spectroscopy
(RP) HPLC - (reverse phase) high performance liquid chromatography

RF - radiofrequency
MRI - magnetic resonance imaging
α-KG - α-ketoglutarate
nOe - nuclear Overhauser effect
α-ABA - L-2-aminobutyric acid
glu - glutamate
gln - glutamine
NAA - N-acetylaspartate
CRS-TLE - carisbamate-treated temporal lobe epilepsy
CRS-ALE - carisbamate-treated absence-like epilepsy

'

Abstract

Temporal lobe epilepsy is the most common type of epilepsy, the latter which has a worldwide occurrence of approximately 1%. As it is also a highly intractable disease, there is a pressing need for the development or improvement of antiepileptic drugs. In this study, the thalamic metabolism in lithium-pilocarpine-treated rats with chronic temporal lobe epilepsy was examined. Additionally, in a previous study, the rats of the same animal model had developed either temporal lobe epilepsy or absence-like epilepsy when treated with the novel antiepileptic drug carisbamate (CRS; RWJ 333369; S-2-O-carbamoyl-1-O-chlorophenyl-ethanol). The metabolic effects of carisbamate on the thalamus of these rats were therefore investigated. In both cases, this was done by using high performance liquid chromatography and nuclear magnetic resonance spectroscopy.

The results found include a disturbed neuronal metabolism in the thalamus of rats with chronic temporal lobe epilepsy, which may be due to either neuronal loss or impaired TCA cycle activity. Furthermore, the treatment with carisbamate was found to have normalising effects on the neuronal metabolism, thus indicating that this drug is neuroprotective. Finally, the metabolic differences between the rats that developed temporal lobe and absence-like epilepsy were limited to a lower level of GABA for the latter. Although the reason for this is not apparent, it may reflect the opposing effects GABA has on the regulation of seizures in the two epilepsy types.

Contents

1. Introduction

1.1 The brain constituents

The brain consists of two cell types: neurons and glia. Whereas the importance of neurons was quickly appreciated, glial cells were considered merely as "glue", binding the nerve cells and holding them in place. Although this structural assignment holds true, today glial cells are recognised as having high levels of complexity and playing many crucial roles for the functioning of the nervous system (1). Glial cells can broadly be categorised into two: micro- and macroglia. The former cells are part of the immune system and may portray phagocytic behaviour if there is need. Macroglia is actually a unifying term for several cell types of the central nervous system (CNS). Astrocytes are the most abundant cells among the macroglia, and form a crucial part of the glial-neuronal-vascular unit. Oligodendrocytes ensure the myelination of neuronal axons in the CNS, thus insulating them and ensuring rapid signalling. Furthermore, ependymal cells line the ventricles and the spinal cord, are connected through tight junctions and help produce the cerebrospinal fluid (CSF) (1,2). All brain cells are protected by the blood-brain barrier (BBB), which is comprised of tight junctions between endothelial cells. This barrier is highly regulatory, preventing macromolecular and toxic substances to enter the brain parenchyma unless they have specific transporters, such as those for glucose. Conversely, molecules that are small and lipophilic may freely diffuse through (3).

1.1.1. Neurons

Neurons are capable of receiving signals from other neurons and transmitting information as electrical signals, or action potentials (AP), either to other neurons or effector organs. This ability distinguishes them from other types of cells, and is the reason for why we are able to sense and respond to the environment. Apart from being unified by the generation of APs, however, neurons have the largest morphological diversity of all cells in the body, both with respect to size and shape. Nevertheless, there are certain physical features the standard neuron encompass, as depicted in Figure 1 (2,4).

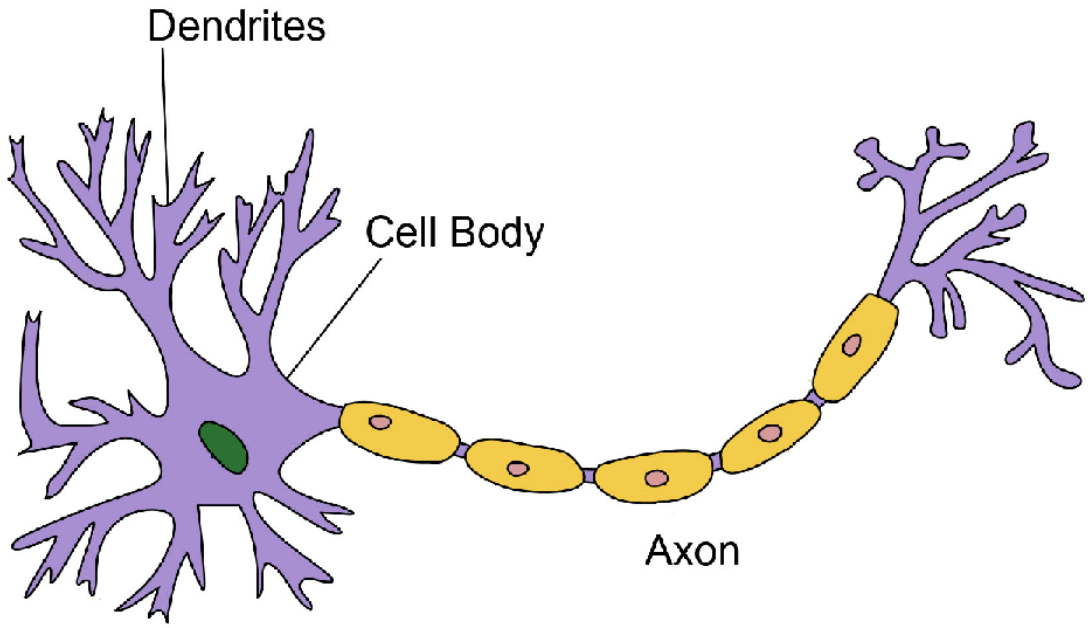

Figure 1. Diagram of a typical neuron. Taken from http://www.explorecuriocity.org/Portals/2/article%20images/neuron.jpg

The cell body, or soma, contains organelles similar to other cell types, that allows for protein synthesis etc. needed for the neuron to survive. Dendrites project from the soma, bringing signals, usually chemical, towards the axon hillock where the AP is generated. The AP is rapidly (up to 100 m/s) propagated down the axon towards the terminal via the influx of Na^+ through voltage-gated Na^+-channels. The speed of propagation is increased with increasing axonal diameter and amount of myelination by oligodendrocytes. Once the AP reaches the terminal, an influx of Ca^{2+} is triggered, which causes the vesicles containing neurotransmitters to dock and release the content into the synapse (2,4,5).

Based on their functions, neurons may be divided into three categories: excitatory, inhibitory and modulatory. Excitatory neurons account for the vast majority of neurons within the CNS, and about 80-90% of these utilise glutamate as the neurotransmitter (2). Glutamate receptors encompass both the ionotropic (iGluRs) and metabotropic (mGluRs) type. The latter mediates slow, but longer lasting responses in the postsynaptic cell, via the activation of a G-protein and subsequent second messenger molecules. Ionotropic glutamate receptors, on the other hand, are ligand-gated and ensure very rapid signalling through the influx of positive ions, Na^+ and/or Ca^{2+}, into the postsynaptic cell (6). If the depolarisation is great enough to reach the threshold, the postsynaptic cell will generate an AP in order to activate other cells (4). Conversely, inhibitory neurons hyperpolarise the postsynaptic cell, usually through γ-aminobutyric acid (GABA). Once GABA is released into the synapse, it activates postsynaptic receptors that allows negative Cl^--ions to enter the cell (5). Inhibitory

neurotransmission is highly important in the CNS, as it helps to modulate neuronal firing and avoid hyperexcitability (2,7)|.

1.1.2. Astrocytes

The name 'astrocyte' was given to these glial cells as the staining targeting glial fibrillary acid proteins (GFAP) characterised them as being star-shaped. It was however discovered that GFAP is only expressed in the larger stem branches, and not at all in the smaller processes, thereby masking the extent of branching in astrocytes (8). The cells are spread around the entire CNS with seemingly non-overlapping domains, and are in close contact with neurons as well as blood vessels and other glial cells (8). In broad terms astrocytes can be divided into two categories based on their morphology: the fibrous, which reside in the white matter tracts, and the protoplasmic located in the gray matter (9). There appears to be some discrepancy regarding the ratio of astrocytes to neurons in the human CNS, with claims of for instance both an equal population (10) and a five-fold difference in the favour of astrocytes (8). Nevertheless, their large number of roles in the physiological brain, as well as frequent signs of dysfunction in the pathological brain, shows that astrocytes undoubtedly are important for the neuronal functioning (8,11).

Astrocytes form part of a tripartite synapse, which also includes pre- and postsynaptic neurons. This, as well as their contact with the vasculature (Figure 2), enables them to provide metabolic support and also gives them a direct control of neuronal signalling. They are crucial for the maintenance of ion, fluid, transmitter and pH homeostasis (8). For example, they have been found to help buffer the increased extracellular levels of potassium (K^+) following neuronal depolarisation. This uptake of K^+ through Kir channels is important, as an altered K^+ homeostasis makes the resting potential more positive, thereby affecting neuronal activation (11). Water homeostasis is maintained through the aquaporin 4 (AQP4) channels distributed throughout astrocytic processes, in particular the ones in contact with blood vessels. This works to prevent conditions such as oedema. Astrocytes have also been found to regulate the local blood flow in the CNS via molecular mediators, as a response to changes in the activity of neurons. This is termed neurovascular coupling (8,12,13). Furthermore, they maintain neurotransmitter homeostasis by mopping up the vast majority of it (e.g. glutamate, GABA and glycine) following neuronal release (8). Another example of an astrocytic task is the conversion of glutamate to glutamine through the enzyme glutamine synthetase (GS), which does not exist in neurons (11). This makes up half of the glutamate-glutamine cycle, which will be discussed in detail later.

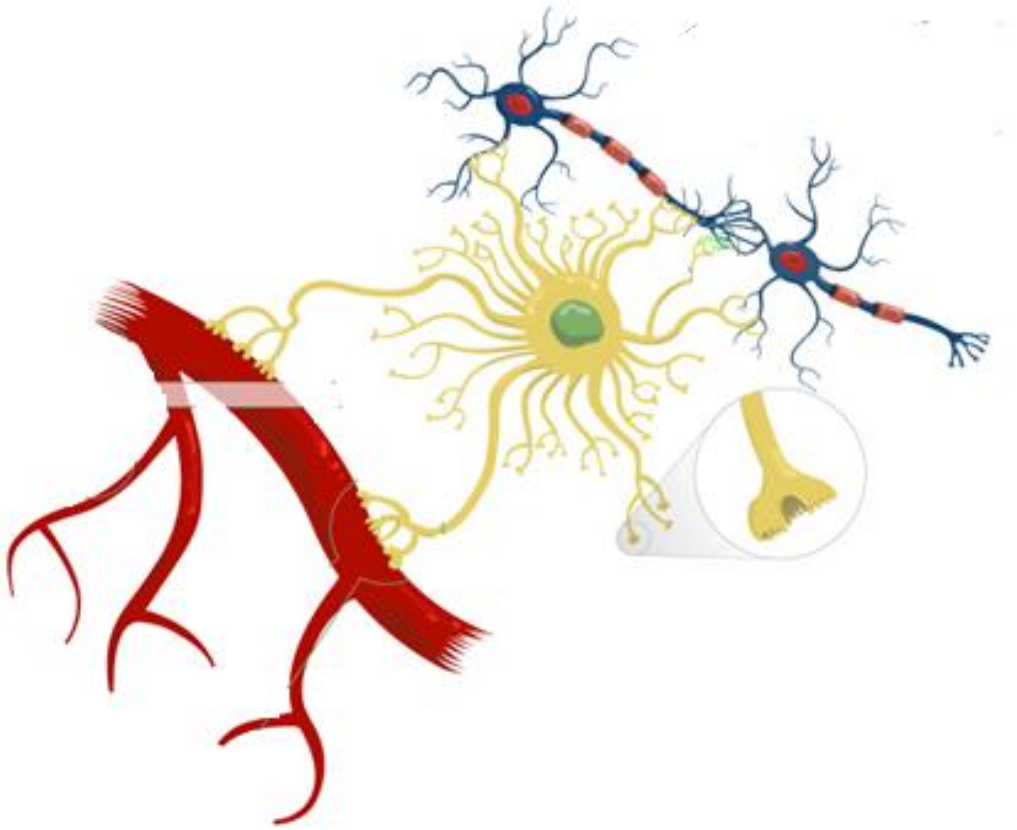

Figure 2. Diagram of the tripartite synapse and the astrocytic contact with the vasculature. The yellow and blue cells are astrocytes and neurons respectively. Adapted from http://learn.genetics.utah.edu/content/addiction/reward/cells.html

1.2 Brain metabolism

1.2.1. Glucose transport into the CNS

The brain needs an enormous amount of energy in order to function. In fact, during rest, a staggering 20% of the total energy is utilised by the brain, despite the fact that it accounts for only 2% of the total body mass (14). Glucose represents the major energy source (more than 90%) for the adult brain. It traverses the BBB, and subsequently into neurons and glia, via facilitation by glucose transporters (GLUT). Out of this class of transporter proteins, it is the GLUT1 and GLUT3 that transport most of the glucose in the brain. There are two isoforms of GLUT1, 55 kDa and 45 kDa, located on the endothelial cells and the perivascular endfeet of astrocytes respectively. GLUT3, on the other hand, is mainly situated on neurons (15).

As mentioned, the transport of glucose into the CNS is crucial for the energy production, which is in the form of the chemical ATP (adenosine triphosphate). However, it is also necessary for the generation of neuromodulators and neurotransmitters, as they are

unable to traverse the BBB (16,17). In order to fulfil these demands, glucose needs to be metabolised once it is inside the cell. This involves anaerobic metabolism, through glycolysis, and subsequent aerobic metabolism. The latter occurs via the tricarboxylic acid (TCA)-cycle and the electron transport chain (16).

1.2.2. Glycolysis

During glycolysis (Figure 3), glucose is catabolised to pyruvate inside the cell cytosol, the rate of which is termed glycolytic flux. This includes ten steps of catalysation by different enzymes, and does not involve the use of oxygen. In the first step hexokinase catalyses the glucose to glucose-6-phosphate (Glc-6-P) conversion. Although ATP is required for this reaction, it is a crucial step because it is irreversible, thus "trapping" glucose and forcing it to be metabolised. Furthermore, this is a branching point in glycolysis, as Glc-6-P also can be utilised for the pentose-phosphate pathway and for generating glycogen (2,18). The hexokinase activity is closely regulated by the concentration of Glc-6-P; if the latter accumulates, hexokinase activity is downregulated (2). In terms of ATP yield, there are two phases of glycolysis: The first phase involves the five-step conversion of one molecule of glucose into two molecules of glyceraldehyde-6-phosphate. This process actually requires the use of two ATP molecules. The second phase, however, which is the conversion of glyceraldehyde-6-phosphate into pyruvate, has a yield of four ATP molecules. The net yield is therefore two ATP molecules, which is an important gain although not sufficient for the brain requirements (18).

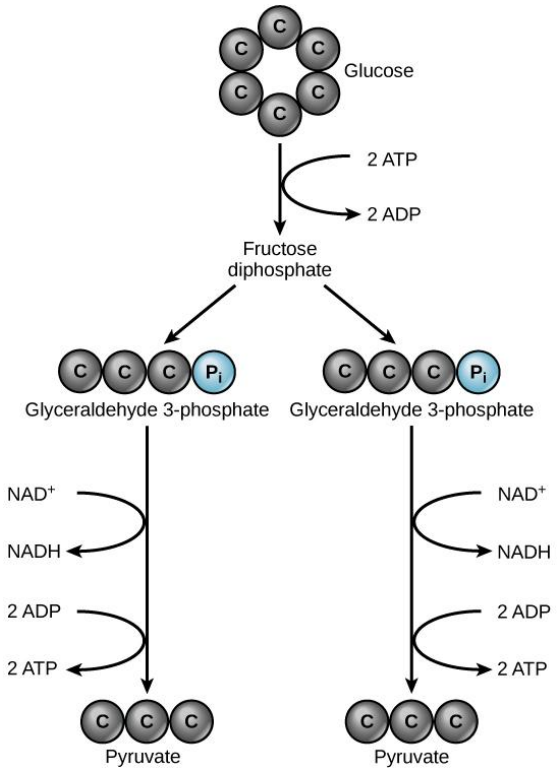

Figure 3. A simplified diagram of glycolysis. The C's represent carbon atoms, and the P_i's represent additions of phosphate. Taken from http://cnx.org/content/m45438/latest/?collection=col11487/latest.

1.2.3. TCA cycle and oxidative phosphorylation

If oxygen is absent, or if the rate of pyruvate oxidation is lower than the glycolytic flux, then pyruvate is converted to lactate in the cytosol via the enzyme lactate dehydrogenase. Another possibility is the formation of alanine, which occurs through alanine transaminase (2). However, if oxygen is present, then entering the TCA-cycle is the most likely fate of pyruvate. This cycle, also called the Krebs and the citric acid cycle, takes place inside the mitochondrial matrix of cells (Figure 4). This means that pyruvate has to be transported across the double membranes of mitochondria, which occurs via proton symport (19). Once inside the matrix, pyruvate is likely to be converted to acetyl-Coenzyme A (acetyl-CoA) via the pyruvate dehydrogenase complex (PDH), which consists of three enzymes. These enzymes regulate the TCA-cycle, as an increase in ATP and acetyl-CoA decreases their activity. The entry of pyruvate into the TCA-cycle via the PDH complex is necessary for its full oxidisation and energy yield (2). However, in astrocytes pyruvate may also be converted to oxaloacetate (OAA) via pyruvate carboxylase (PC). This is an equally important reaction, as it replenishes intermediates of the TCA-cycle and leads to the de novo biosynthesis of amino acids such as glutamate and glutamine (2,20). In this anaplerotic process, PC adds a carbon to the backbone of pyruvate to form OAA. The latter is then rapidly removed through a condensation reaction with acetyl-CoA for the formation of a novel molecule of citrate (2).

The full oxidation of one glucose molecule gives this equation:

$$C_6H_{12}O_6 + 6O_2 \longrightarrow 6CO_2 + 6H_2O$$

For each glucose molecule there are two carbons lost from the conversion of pyruvate to acetyl-CoA. Furthermore, one glucose molecule leads to two rounds of the TCA-cycle, from which another four carbons are lost. In terms of energy yield, however, two rounds of the TCA-cycle produces two molecules of GTP, which is related to ATP and may produce ATP by transferring a phosphate group to ADP. Furthermore, six molecules of NADH and two molecules of $FADH_2$ are also generated, all of which carry high-energy electrons. When these and the NADH derived from glycolysis are subjected to oxidative phosphorylation, the electrons are carried through the electron transport chain embedded in the inner mitochondrial membrane. As a result of this, H^+-ions are pumped out to the intermembrane space, generating a proton gradient which allows the ATPase to phosphorylate ADP. The theoretical energy yield from one glucose molecule is 38 ATP; however, due to some production of lactate and alanine, as well as different uses of the protons, the actual yield is likely to be lower (2,21).

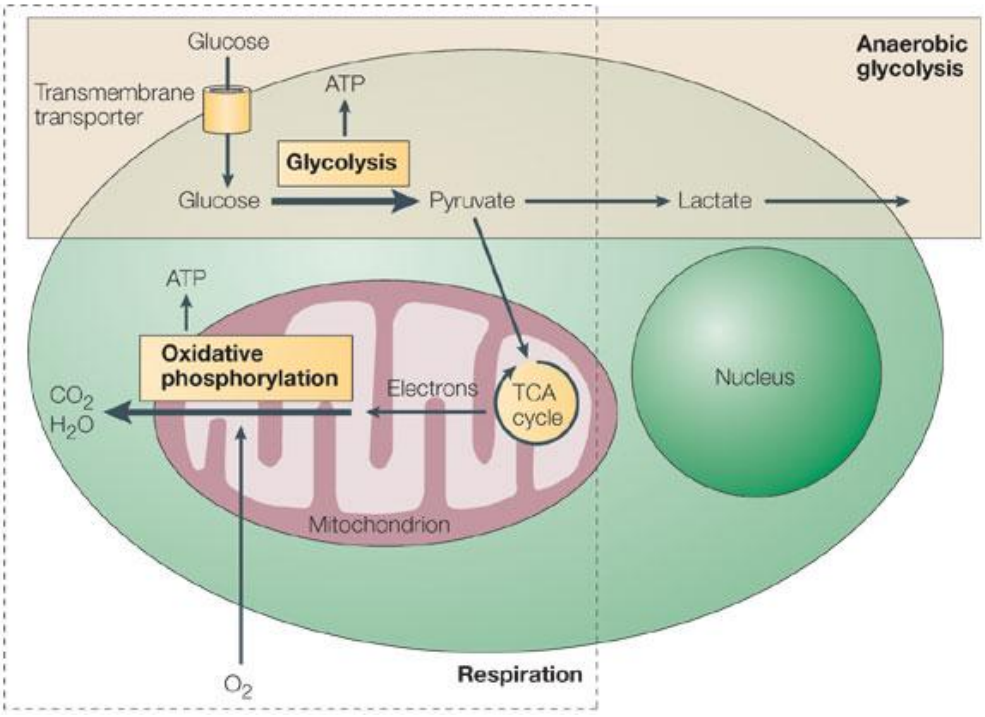

Figure 4. A simplified diagram of the cell metabolism. ATP=adenosine triphosphate. Adapted from Sitkovsky and Lukashev (22)**.**

1.2.4 Compartmentation and neuronal-astrocytic interactions

Although glucose metabolism occurs in all brain cells, there are many differences regarding the metabolic rates, sites of synthesis and metabolite uptake and concentrations. The result of this is of course that brain cells are highly dependent on each other, with one example being the astrocytic PC forming intermediates for brain TCA-cycles. Furthermore, recent research indicates that the uptake and utilisation of glucose increases dramatically in astrocytes, but remains the same in neurons during intense neuronal activation (23). This is in contrast to resting conditions, during which the overall uptake of glucose has been shown to be approximately equal between neurons and astrocytes (24). The reason for this activation has been linked to neuronal signalling: As astrocytes remove glutamate from the synaptic cleft, they take up Na^+ in the process, thereby increasing the intracellular Na^+-concentration. As a result of this, the Na^+/K^+-ATPase is activated in order to pump out Na^+ and restore its equilibrium, which is an energy demanding process (25).

In spite of this increase in glycolysis in astrocytes during neuronal activation, they are only estimated to account for approximately 30% of the brain oxidative phosphorylation (26). It has therefore been proposed that a majority of the glycolytic end product is shuttled to the neurons in the form of lactate for the entry into the neuronal TCA-cycle (27). Direct *in vivo* evidence for this is however lacking and difficult to obtain, thereby making the lactate shuttle hypothesis controversial (2).

The evidence regarding another type of interaction between neurons and astrocytes, namely the glutamate-glutamine-cycle, is more solid. In both cell types, glutamate can be reversibly generated from the TCA-cycle intermediate α-ketoglutarate via glutamate dehydrogenase (GDH) or several aminotransferases. It may also be generated from glutamine; however, this only occurs in neurons, as astrocytes may lack the enzyme phosphate-activated glutaminase (PAG) required for this conversion. Conversely, the synthesis of glutamine from glutamate can only take place in astrocytes, since the required enzyme, GS, is confined to these glial cells (2). The glutamate-glutamine cycle makes up a major metabolic pathway in the brain; after all, glutamate is the main neurotransmitter and nearly all of it is removed from the synapse through glutamate transporters on astrocytic membranes. Some of the glutamate is then fed into the astroglial TCA-cycle via α-ketoglutarate. Nevertheless, the majority is converted to glutamine before it is released from the astrocytes and taken up by presynaptic neurons via systems N and A transporters respectively. Once inside the neurons, glutamine is converted back to glutamate and either transported into vesicles, or fed into the TCA-cycle

(28,29). If the neuron is inhibitory, however, glutamate may be further converted to GABA via glutamate decarboxylase (GAD), taken up into vesicles, before being released into the synapse (2).

1.2.5. Acetate metabolism in the CNS

One method of studying astrocytic metabolism in particular, as well as astrocytic-neuronal interactions, is by utilising acetate. This is because acetate uptake mainly occurs by astrocytes, and very little by neurons (2,30,31). Transport into the cells is rapid, and occurs via monocarboxylic acid transporters (MCTs) located on the astrocytic cell membranes. This uptake is stimulated by glutamate and reduced by elevated intracellular concentrations of Ca^{2+} and Na^{+}. Once inside, acetate is converted to acetyl-CoA, and may thus enter the TCA-cycle directly in contrast to glucose, which has to go through glycolysis (30,31).

1.3. Epilepsy

In the normal brain, there is a fine balance between neuronal excitation and inhibition, thus preventing abnormal electrical activity (32). However, if this balance is disrupted, it may lead to the hyperactivity and hypersynchrony that characterises epileptic seizures. It has been highly challenging to agree on the definition of epilepsy, especially since epilepsy is considered a family of disorders with a diverse range of possible underlying causes (for simplicity I will only refer to it as a single disorder) (33). In order to establish the presence of epilepsy, however, a person must have an epileptogenic abnormality that is persistent and capable of causing spontaneous seizures. In other words, an acute seizure caused by a momentary insult or loss of homeostasis, is not defined as epilepsy (34).

The estimated occurrence of epilepsy worldwide is approximately 1%, thereby making it one of the most common neurological disorders (35). The disorder may either be 'idiopathic' (primary) or 'symptomatic' (secondary). Idiopathic epilepsy is not related to other pathologies in the brain, but is genetically transmitted and age-related. Symptomatic epilepsy, on the other hand, arises from another brain pathology that may either be genetic or acquired. If the cause of epilepsy is unknown, it is often referred to as 'cryptogenic' (36). Though these terms are widely utilised, it has lately been suggested that they be changed to 'genetic', 'structural/metabolic' and 'unknown' respectively (37). Epilepsy may be further categorised depending on the origin of the seizures, although there are cases of epilepsy that do not fall into only one of the categories. Nevertheless, the seizures are generalised if the onset is in both hemispheres. This accounts for approximately 40% of all cases of adult epilepsy. If the onset of the seizures is in one part of the brain, the seizure is focal, although it may become

secondarily generalised (36,38,39). Additionally, the seizures may be termed either complex or simple if consciousness is lost or retained, respectively (36).

1.3.1 Temporal lobe epilepsy

Temporal lobe epilepsy (TLE) is the most common type of all epilepsies. According to a study performed by Semah et al. (40), epileptic seizures with a focal origin account for approximately 60% of all adult epileptic seizures, of which about two thirds originate in the temporal lobe. Moreover, TLE is the most frequently intractable type of epilepsy that patients seek surgery for, although the surgery is unsuccessful in 20-30% of the patients (41). It is divided into two subgroups: mesial temporal lobe epilepsy (MTLE), which accounts for about 2/3 of the TLEs and which is when the seizure onset site is in the amygdalo-hippocampal area; and lateral temporal lobe epilepsy (LTLE), where the seizures start in the neocortex (39,42). The LTLE will not be further discussed in this thesis, and MTLE will be written as TLE from now on.

TLE is a symptomatic, chronic and progressive type of epilepsy. In most patients it is caused by an initial precipitating injury (IPI), and in most cases this IPI entails a history of febrile seizures occurring within the first 4-5 years of life. Other types of IPI, such as strokes, infections or status epilepticus (SE), may also occur, though on average later in life compared to the febrile seizures (43,44). The IPI is then followed by a latency period of around 5-10 years, during which there are no symptoms but the brain is undergoing a cascade of epileptogenic changes, before eventually spontaneous seizures occur (45,46). TLE patients often respond to antiepileptic drugs (AEDs) in the beginning after the latency period. However, during adolescence or later, the seizures usually recur and become intractable to the treatment (36).

A very typical form of pathophysiology in TLE is hippocampal sclerosis. This is a type of lesion in the dentate gyrus, CA1 and CA3 regions of the hippocampus caused by loss of pyramidal neurons and astrogliosis (proliferation of astrocytes) (45,46). Neurogenesis of granule cells within the dentate gyrus, in addition to sprouting of their axons, termed 'mossy fibres', are also characteristics commonly seen in TLE. It has been suggested that the latter increases the hippocampal excitability and thus contributes to the progression of the disorder (45–47).

The seizures of TLE usually begin with an aura. In most cases, the symptoms are autonomic or psychic, such as a feeling of epigastric rising, of fear or a sensation of smell or

taste. The seizure itself is often complex and initiates with arrest of movement and stare. Automatisms, such as lip smacking, as well as posturing of the contralateral arm, are also frequent. After the seizure, the patient is often disoriented with a loss of recent memory, in particular regarding the seizure. If the seizure onset is in the hemisphere where language is dominant, dysphasia may occur for up to several minutes (45).

1.3.2 The absence epilepsies

Absence seizures, previously called petit mal seizures, can be divided into two categories: typical and atypical (48). Patients suffering from typical absence seizures show characteristic clinical and electroencephalogram (EEG) expression both during and between the seizures. The ictal EEG recordings often show generalised 3-4 Hz spike wave discharges, whereas the background EEG in between seizures usually is normal. Consciousness is abruptly impaired for the duration of the seizure, usually between 2-20 seconds. During this time, the patient stops his preictal activity and is unresponsive. However, the activity is resumed after the seizure with the patient being unaware of what just happened. Further clinical signs include automatisms, such as lip licking and aimless walking; small clonic jerks of either facial or other muscles; tonic (stiffening) or atonic (relaxing) posturing, and autonomic symptoms, such as sweating or flushing (48). The atypical absence seizures are more heterogeneous. They often include bilateral but asymmetrical abnormalities, with irregular spike-and-slow-wave complexes. Furthermore, the interictal background expression is usually abnormal (48)

Typical absence seizures are characteristic for several types of epileptic syndromes. The International League Against Epilepsy has recognised four types, namely childhood absence epilepsy (CAE), juvenile absence epilepsy (JAE), juvenile myoclonic epilepsy (JME) and myoclonic absence epilepsy (MAE) (42). All of these types have generalised seizures; however, whereas the former three are genetically determined and idiopathic, the MAE is classified as symptomatic or cryptogenic. CAE and JAE are similar in the sense that absence is the main seizure type, although the seizures are much more frequent in CAE. The onset is early in life for both types, before and after 10 years of age for CAE and JAE respectively. However, whereas CAE patients often have a good response to certain antiepileptic drugs and remit before 12 years of age, JAE patients may need treatment for the rest of their lives (42,49). For JME patients, more than one-third experience typical absence seizures, whereas almost all have generalised tonic-clonic seizures. Usually the absence seizures appear at adolescence or earlier, whereas the myoclonic jerks and tonic-clonic seizures appear around 16 years of age. The seizures may become less severe with age, but they will probably

continue for life. The last type, MAE, is a rare syndrome. The absence seizures, which first appear around 7 years of age and occur several times per day, are often accompanied with tonic contraction and clonic jerks, which the patient may be aware of. This type of epilepsy is often refractory to antiepileptic drugs (42,49).

1.3.3. The thalamus and its involvement in TLE and the absence epilepsies

The thalamus (Figure 5), meaning "inner chamber" in Greek, is often called the "gate to the cortex" due to its function as a major relay centre for input to the entire cortex (50). It is bilaterally symmetrical, with two walnut-shaped lobes, and is located in the diencephalon on either side of the third ventricle (51). There are two major components of the thalamus, namely the *dorsal thalamus*, which is further divided into the anterior, medial, ventrolateral and posterior nuclear groups containing several subnuclei; and the *ventral thalamus*, in which the major portion comprises the thalamic reticular nucleus (51,52). Moreover, there are three main cell types within the thalamus: In the dorsal portion there are both glutamatergic relay neurons and GABAergic interneurons, although in several animal species, such as rodents, the latter is more or less absent in nearly all thalamic nuclei (52). The thalamic reticular nucleus, on the other hand, contains only GABAergic reticular neurons which surround the dorsal thalamus like a sheath (53).

The relay neurons of the dorsal thalamus receive typically sensory information from "drivers", such as optic nerve fibres and cortical layer 5 neurons. This accounts for between 5-10% of the input. However, the majority of the information is derived from "modulators", mainly from the neocortex or the brainstem, which may slightly modify the nature of the relay. This occurs either directly, or by acting on intermediate interneurons or reticular neurons (54). Relay neurons may then send first or higher order information to layer 4 of the neocortex, which is processed, returned to the relay neurons from layer 5 of the neocortex, and subsequently updated for every turn of the thalamocortical loop. However, relay neurons may also project to the basal ganglia, thus forming part of the cortico-striatal-thalamocortical loop (55). GABAergic neurons are highly abundant in human thalami (e.g. between 35-40% of the neuronal population within the lateral geniculate nucleus, ventrobasal complex, ventral anterior and ventrolateral nucleus), and provide a strong regulation of the thalamic activity. In fact, the reticular neurons receive input from thalamocortical, corticothalamic and modulatory fibres, but they only project to the dorsal thalamus. Therefore, they may inhibit the latter via both feedforward and feedback mechanisms (52,53).

Since the thalamus is such a central organ in the brain, with a wide array of connections, it is also often involved in, or affected by, different brain disorders. For example, although TLE is mainly associated with a dysfunction of hippocampal and limbic structures, there have been several studies reporting thalamic pathophysiology such as atrophy (56,57). Although the volume reduction has been shown to be bilateral, there is generally a larger decrease in the lobe ipsilateral to the focus of the seizure (57). This loss of volume has also been linked to other dysfunctions, such as cognitive impairment (58). Furthermore, it has been proposed that the thalamus is involved in the modulation of temporal lobe seizures through hyperexcitable connections between the atrophic midline thalamic nuclei and limbic structures (59). It has also been suggested that the seizure focus may at times include the midline thalamic nuclei, as well as the amygala and hippocampus (59).

In terms of the absence epilepsies, however, the involvement of the thalamus is more clear, as it has been established that the seizures originate within the thalamocortical loop. More specifically, it has been demonstrated that the generation of absence seizures are due to a thalamic organisation of the cortical excitatory input into an ictal discharge (60,61). Furthermore, GABAergic neurons within the thalamus, in particular the thalamic reticular nucleus, have been found to generate oscillations that may play a role in the generation of these absence seizures (62).

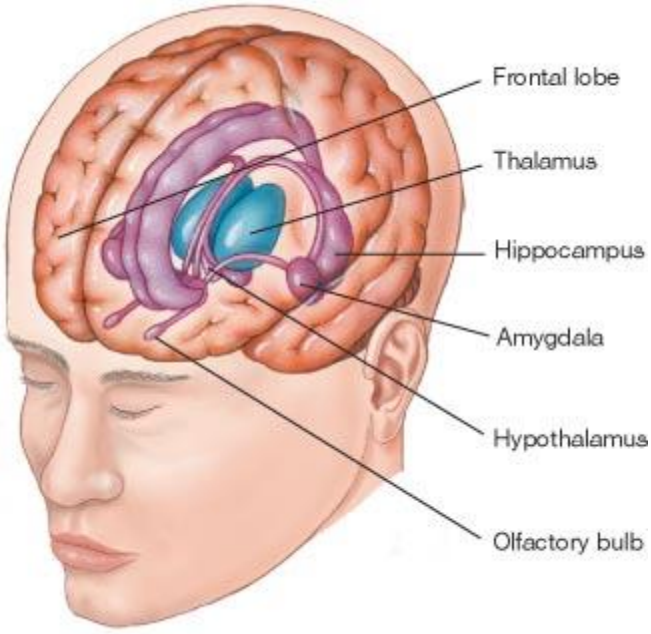

Figure 5. The location of the thalamus. Adapted from http://cwx.prenhall.com/bookbind/pubbooks/morris5/medialib/images/F02_09.jpg

1.3.4 Cell metabolism in epilepsy

As previously mentioned, seizures are a result of hyperactivation and hypersynchrony, the reason for which has been linked to a disruption in the balance between excitation and inhibition. Since the main excitatory and inhibitory neurotransmitters are glutamate and GABA respectively, the mode of action for many AEDs include blocking the activity of the former and promoting the activity of the latter (63,64). Nonetheless, it has also been reported that excess GABA may cause seizures, for example within the thalamocortical loop (65).

In terms of TLE, it is well established that the majority of patients have interictal hypometabolism in the region ipsilateral to the seizure focus (e.g. (66,67)). Conversely, hypermetabolism has been demonstrated during the ictal phase in the kainic acid (KA) rat model of TLE (68). These results are in contrast to the increased ictal and decreased interictal metabolism that has been reported in the Genetic Absence Epilepsy Rats from Strasbourg (GAERS) (69,70).

1.3.5 Animal models of temporal lobe epilepsy

The AEDs used for treating TLE today actually only work by suppressing the seizures. In other words, they target the symptoms, rather than trying to cure the actual disorder. Furthermore, nearly 40% of TLE patients do not respond to AEDs at all. It is therefore clear that further research is required to learn more about the mechanisms of epileptogenesis, as well as the processes causing pharmacoresistance. In addition, disease-altering therapies should be developed to prevent the progression of TLE (71–73). The best way to do this, is to utilise animal models that in the best way possible duplicate this disorder in humans, thus they need to possess certain characteristics. For instance, as TLE mostly is a symptomatic disorder, the animals should be healthy before epilepsy is induced either chemically or electrically (72,74). Furthermore, they should exhibit hippocampal sclerosis as well as chronic seizures that originate from the temporal lobe and progress over time. A latency period is also preferential between the initial insult and the occurrence of spontaneous seizures (74).

1.3.5.1 The lithium-pilocarpine model

The rodent model that has become one of the most widely utilised for MTLE research, is the lithium-pilocarpine model, as it exhibits all of the aforementioned characteristics (74). The chemical pilocarpine, which is a muscarinic acetylcholine receptor agonist, is injected in order to induce SE corresponding to the IPI. On a molecular level, this occurs via the activation of muscarinic, and subsequently *N*-Methyl-$_D$-aspartate (NMDA) receptors, causing rapid neural

depolarisation, lasting increases in extracellular glutamate and GABA, as well as excitotoxicity (75). The post injection symptoms include salivation, scratching, grooming, wet-dog shakes and chewing, prior to the onset of the seizures. Lithium chloride is administered prior to the pilocarpine injection in order to reduce the amount of the latter and thereby decrease the peripheral brain damages, as it potentiates the effects of pilocarpine (75–78). In the case of rats, after the SE is interrupted after around 90 to 120 minutes, a latency period ensues, which typically lasts for about 3-4 weeks (72,79). The animals have normal EEG activity and behaviour during this period. Furthermore, while the mitochondrial H_2O_2 production during the SE is abnormally high, leading to oxidative stress, during latency these levels return back to normal (74,80). Several pathophysiological events are however believed to occur during the latent phase that later lead to the spontaneous recurrent seizures (74).

1.3.6 Antiepileptic drugs

There has been a marked increase in the development of drugs to treat epileptic seizures for the past 15 years, which becomes clear when looking at the number of newly approved AEDs in the United States alone: since AEDs first became available in the 1960s, and up until 1993, there were only nine AEDs that had been approved by the Food and Drug Administration (FDA). During a subsequent period of 12 years, the number rose to include another ten drugs, whereas there were a total of five AEDs approved only between 2009 and 2011 (64). The mode of action for most of these are believed to include several mechanisms, such as the modulation of sodium or calcium associated channels or interacting with GABA receptors in order to increase neuronal inhibition (64,81). Although the quality of the new AEDs (developed after 1993) has improved considerably compared to the old ones, there is still no drug available that consistently can cure the seizures of all patients, and side effects remain a problem (81).

1.3.6.1 Carisbamate

Carisbamate (CRS; RWJ 333369; S-2-O-carbamoyl-1-O-chlorophenyl-ethanol) (Figure 6) is a neuromodulator and an analogue to the already approved AED felbamate. Its mechanism of action is still not yet known; however, it is thought to block voltage-gated Na^+-channels as well as some Ca^{2+}-channels, and also activate Cl^--conductances either pre- or postsynaptically (82,83). The drug has previously been shown to have a broad spectrum of anticonvulsant activity in different types of animal models. This includes, but is not limited to, the maximal electroshock, pentylenetetrazol, bicuculline, picrotoxin, audiogenic and lithium-pilocarpine

seizure models (84). In the latter model, it was found that an injection of CRS i.p. prior to or i.v. after the administration of pilocarpine either prevented or interrupted the occurrence of SE (84). Furthermore, CRS has been shown to decrease the frequency of seizures and spike-and-wave discharges (SWDs) in the rat kainate and GAERS models respectively (85,86).

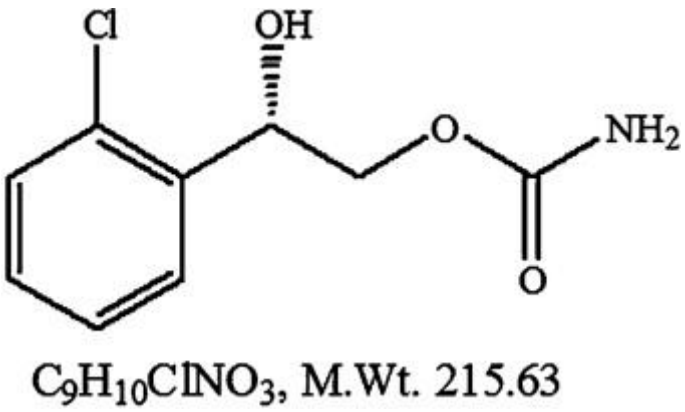

$C_9H_{10}ClNO_3$, M.Wt. 215.63

Figure 6. The molecular structure, formula and weight of carisbamate.

Previously, François et al. (76) investigated the effects of CRS on neuroprotection and the occurrence of spontaneous seizures in rats with lithium-pilocarpine-induced temporal lobe epilepsy. In this study it was found that, at the two highest doses of CRS (90 mg/kg and 120 mg/kg), there was significant neuroprotection compared to the control rats treated with diazepam. This was in particular in the regions of Ammon's horn of the hippocampus, piriform and entorhinal cortices, thalamus and amygdala. Furthermore, the rats treated with these doses of CRS showed three different types of responses in relation to seizures: Two groups developed motor seizures after a period of short and prolonged latency, whereas the third group (45%) had no motor seizures for more than 240 days, but rather showed spike-and-wave discharges (SWDs) that are characteristic to absence seizures.

The effects of CRS in clinical trials have however been more inconsistent. It was shown to be efficacious at certain doses in a Phase IIb study; however, this was only the case in one out of two Phase III studies lasting for a 12 week period. Furthermore, yet another Phase III study failed to show a statistical significance in the CRS treated group compared to the group receiving placebo (87). Because of this lack of consistent efficacy, the submissions for its new drug application (NDA) and medical authorization application (MAA) were withdrawn early 2010, with a subsequent discontinuation of the clinical program in epilepsy (83,87). However, the beneficial effects in animal models are so clear, thus further animal

studies are warranted to investigate which mechanisms are responsible for this and how they can be mimicked by more effective drugs in humans.

1.4 Aims

Intractable epilepsy remains a major problem, therefore it is necessary to develop new, and/or improve already existing, AEDs. As previously mentioned, CRS has been shown to have neuroprotective and disease-modifying effects on rodents (e.g (76)). However, as the mode of action and metabolic effects of CRS are not yet known, it is of interest to develop a better understanding of this. In this thesis, the thalamic metabolism in the lithium-pilocarpine rat model with and without CRS treatment was investigated. More specifically, ^{1}H-NMRS, ^{13}C-NMRS and HPLC were used to address the following questions:

1. How does chronic TLE affect the neuronal and astrocytic metabolism and interaction in the thalamus?
2. How does CRS affect the neuronal and astrocytic metabolism in the thalamus of rats injected with lithium-chloride and pilocarpine?
3. What are the thalamic metabolic differences between the CRS-treated rats that developed TLE and absence-like epilepsy?

2. Theoretical background of methods

2.1 HPLC

High performance liquid chromatography, or HPLC, is a technique that arose in the late 1960s to separate the components of a mixture, such as amino acids in cell extracts (74). It contains a column with a densely packed stationary phase, for instance silica, as well as a liquid mobile phase, which is eluted from the column along with the sample. The components of the sample have different levels of interactions with the stationary phase, thus producing bands of separation and different retention times as it runs through (89). In most cases, including this experiment, this separation is based on polarity. This means that the more non-polar constituents are attracted to the non-polar stationary phase, and are thus retained within the column. Conversely, the polar constituents are attracted to the polar mobile phase being pumped through, and will therefore elute faster (90). The use of a lipophilic stationary phase and hydrophilic mobile phase makes it into a reversed-phase (RP) HPLC, which is the most common type of HPLC today. By utilising a solvent gradient, where the mobile phase becomes decreasingly polar, the total time period needed to elute all components can be decreased (90,91). Finally, the eluents pass through a detector for their identification and quantification. Today, there are many different detector systems available, for example those based on UV-light or fluorescence (92). If the latter is used, as in this experiment, a derivatisation agent is required to render the components fluorescent. The signal is then directly proportional to their concentration, which is determined by the use of standard curves.

HPLC has several advantages over older types of liquid chromatography, primarily because of the use of a high pressure pump where the others rely on gravity alone as the driving force through the column. This allows for the use of smaller stationary phase particles, which, in addition to the faster flow rate, improves the efficiency and resolution through decreased retention times as well as less band broadening (88,93).

2.2 NMR Spectroscopy

In 1945, two independent research groups led by Felix Bloch and Edward Purcell showed that electromagnetic radiation is absorbed by nuclei if they are placed in a strong magnetic field. Their advances in the development of NMR spectroscopy later earned the two physicists a joint Nobel Prize in Physics (94). NMR deals with frequencies appearing within the radiofrequency (RF) range, which are unusually low compared to other types of spectroscopy.

The fact that this range is non-ionising also makes it ideal for *in vivo* use, in the form of MR imaging (MRI) (95).

Isotopes need to have nuclei possessing a magnetic dipole moment in order to be NMR active. This magnetism is generated from a combination of the positive charge of the nuclei as well as their spin angular momentum, the latter which is present unless the number of both protons and neutrons is even. ^{1}H and ^{13}C are examples of isotopes that possess such a spin property, with a spin quantum number of ½ (94).

Individual nuclei that are NMR active can be characterised as small magnetisation vectors that are randomly oriented in the absence of an external magnetic field, $\boldsymbol{B_0}$. However, if an external magnetic field is applied, there are two things that occur:

- The magnetisation vectors will adopt specific orientations, which, in the case of ^{1}H and ^{13}C, are either parallel (low energy state) or antiparallel (high energy state) to the external field (95).
- The magnetisation vectors start to precess about the external field, at a frequency characteristic for that isotope (96).

The proportion of nuclei residing in the two states can be calculated using the Boltzmann equation:

$$\frac{N_\alpha}{N_\beta} = \mathrm{e}^{\frac{\Delta E}{kT}}$$

Figure 7. $\boldsymbol{N_\alpha}$ and $\boldsymbol{N_\beta}$ represent the number of nuclei residing in the low and the high energy state respectively; $\boldsymbol{\Delta E}$ is the energy gap between the two states; $\boldsymbol{k}$ is the Boltzmann constant and $\boldsymbol{T}$ is the absolute temperature (97).

This equation is really important because it is the excess nuclei in the low energy state that are able to absorb the electromagnetic radiation applied as a pulse. This ratio can be increased, in theory, by either increasing the force of the B_0, which would also increase the energy gap between the two states, or by decreasing the thermal energy (98). The latter is because too much thermal motion of the molecules causes the magnetic moments to have random orientations (95).

The precession frequency, also called the *Larmor frequency*, is directly proportional to the force of B_0, and can be calculated using this equation:

$$\boldsymbol{\omega_0 = \gamma B_0}$$

Figure 8. γ represents the gyromagnetic ratio of the nuclei (96).

In order for the nuclei to be able to absorb the energy applied, the pulse needs to be at the Larmor frequency specific for that isotope. Additionally, it has to be applied at an angle perpendicular to that of the magnetisation vectors, i.e. along the XY-plane. This makes them precess phase coherently, and causes their orientation, overall represented by the *bulk magnetisation vector*, to change. As the nuclei relax, energy is released which can be detected by a coil surrounding the sample (98,99).

The relaxation processes that occur after the radiofrequency pulse has been removed involve the recovery of the longitudinal bulk magnetisation vector ($T_{1,}$ or spin-lattice), and the loss of phase coherence along the horizontal plane ($T_{2,}$ or spin-spin). The occurrence of the latter might seem strange, since nuclei of a specific isotope are phase coherent after a pulse and seemingly precess at the same Larmor frequency. However, the force of the B_0 is weakened by the shielding effect of surrounding electrons, meaning that the effective magnetic field at the site of the nuclei depends on the electronegativity of the neighbouring atoms. This is what gives rise to slightly different precession frequencies, which again is the reason for why peaks appear at different regions of the NMR spectra, displayed as *chemical shifts* (94,100).

2.2.1. ^{1}H-NMRS

With a natural abundance of 99.98% and a high gyromagnetic ratio, ^{1}H is the most sensitive isotope that can be utilised in NMR. Furthermore, its presence in nearly all metabolites implicates that ^{1}H NMR is a good technique for metabolite identification and quantification (101).

2.2.2. ^{13}C-NMRS

In contrast to ^{1}H, the natural abundance of ^{13}C is only about 1.1%. Additionally, the gyromagnetic ratio is much lower, meaning that ^{13}C NMR is a highly insensitive technique. However, this method can provide invaluable information about metabolic pathways, so it is still highly utilised. One way to overcome the insensitivity is to inject the animal with ^{13}C enriched precursors to increase the signal-to-noise ratio (101).

If the isotopomers contain two neighbouring ^{13}C isotopes, there will be a *homonuclear spin-spin coupling* characterised by peak splitting. This is because one isotope will affect the magnetic field of the other isotope. If the distance between the two peaks comprising the doublet is approximately 54 Hz, then one of the ^{13}C isotopes belong to a carboxylic acid group. For example, since this is the case for C1 of glutamate, glutamine and GABA, the split

between the C1 and C2 will be approximately 54 Hz. If neither of the ^{13}C isotopes are part of a carboxylic acid group, which is the case for C2 and C3 of glutamate, glutamine and GABA, the distance between the peaks of the C2-C3 doublet will be approximately 34 Hz (102).

The magnetic field of one isotope may also affect the magnetic field of a different neighbouring isotope, the term of which is *heteronuclear spin-spin coupling.* In this study, the relevant isotopes are ^{1}H and ^{13}C. To avoid this, it is possible to decouple the ^{13}C-NMRS spectra by simultaneously irradiating the proton resonances. In addition to making the spectra easier to read due to a reduction of peaks, there will also be an increased signal-to-noise ratio. Additionally, this ratio is further changed (mostly increased) as the signal emitted from ^{13}C isotopes during relaxation is affected by the irradiation of protons. This is termed the *nuclear Overhauser effect* (nOe), and needs to be corrected for through calculations (103).

2.2.3. Labelling patterns from [1-^{13}C]glucose

At rest, [1-^{13}C]glucose may enter both neurons and astrocytes at equal amounts (24), though there is controversy about this and diversity due to brain area is expected. [1-^{13}C]glucose is oxidised to form one mole of unlabelled and one of [3-^{13}C]pyruvate. The latter may be converted to [3-^{13}C]alanine or [3-^{13}C]lactate, or enter the TCA cycle. In neurons, this has to happen via the PDH-complex, forming [2-^{13}C]acetyl-CoA, which can condense with unlabelled OAA to form [4-^{13}C]α-ketoglutarate (α-KG). The latter may leave the TCA-cycle to form [4-^{13}C]glutamate and subsequently [4-^{13}C]glutamine (in astrocytes) or [2-^{13}C]GABA in GABAergic neurons (Figure 9, shown in red). If [4-^{13}C]α-KG remains in the TCA-cycle, it is further oxidised to equal amounts of [2-^{13}C]- or [3-^{13}C]succinate, and subsequently [2-^{13}C]- or [3-^{13}C]OAA. The latter two may then be transaminated to yield [2-^{13}C]- or [3-^{13}C]aspartate, or they may continue into a second turn of the TCA-cycle. If this occurs via a condensation reaction with unlabelled acetyl-CoA, then [2-^{13}C]- or [3-^{13}C]α-KG is formed in equal amounts, which may leave the TCA-cycle by forming [2-^{13}C]- or [3-^{13}C]glutamate and thereafter glutamine, or [3-^{13}C]- or [4-^{13}C]GABA in the respective cell types. If [2-^{13}C]- or [3-^{13}C]OAA is condensed with [2-^{13}C]acetyl-CoA, however, it will yield [2,4-^{13}C]- or [3,4-^{13}C]α-KG, with a subsequent formation of [2,4-^{13}C]- or [3,4-^{13}C]glutamate or glutamine, or [2,4-^{13}C]- or [2,3-^{13}C]GABA.

In astrocytes, [3-^{13}C]pyruvate may also enter the TCA-cycle via PC for the formation of [2-^{13}C]OAA. The latter can then condense with unlabelled acetyl-CoA, which will yield [2-

[13]C]α-KG and which will either remain in the TCA-cycle or leave it, producing [2-[13]C]glutamate and subsequently [2-[13]C]glutamine, or [4-[13]C]GABA (Figure 9**,** shown in blue**)**.

2.2.4. Labelling patterns from [1,2-[13]C]acetate

[1,2-[13]C]Acetate enters the TCA-cycle via the conversion into [1,2-[13]C]acetyl-CoA and subsequent condensation with unlabelled OAA to yield [4,5-[13]C]α-KG. The latter may then leave the TCA-cycle and produce [4,5-[13]C]glutamate and subsequently [4,5-[13]C]glutamine, or [1,2-[13]C]GABA (Figure 9, shown in green). If not, it may feed into a second round of the TCA-cycle via [1,2-[13]C]- or [3,4-[13]C]OAA. The former yields [3-[13]C]α-KG, glutamate, glutamine or GABA if condensed with unlabelled acetyl-CoA, whereas the latter yields [1,2-[13]C]α-KG, glutamate or glutamine, or [4-[13]C]GABA. It is also possible that the [1,2-[13]C]- or [3,4-[13]C]OAA is condensed with [1,2-[13]C]acetyl-CoA for the second turn; however, this labelling pattern is too complex and is not present in this study in detectable amount, and will therefore not be discussed in this thesis.

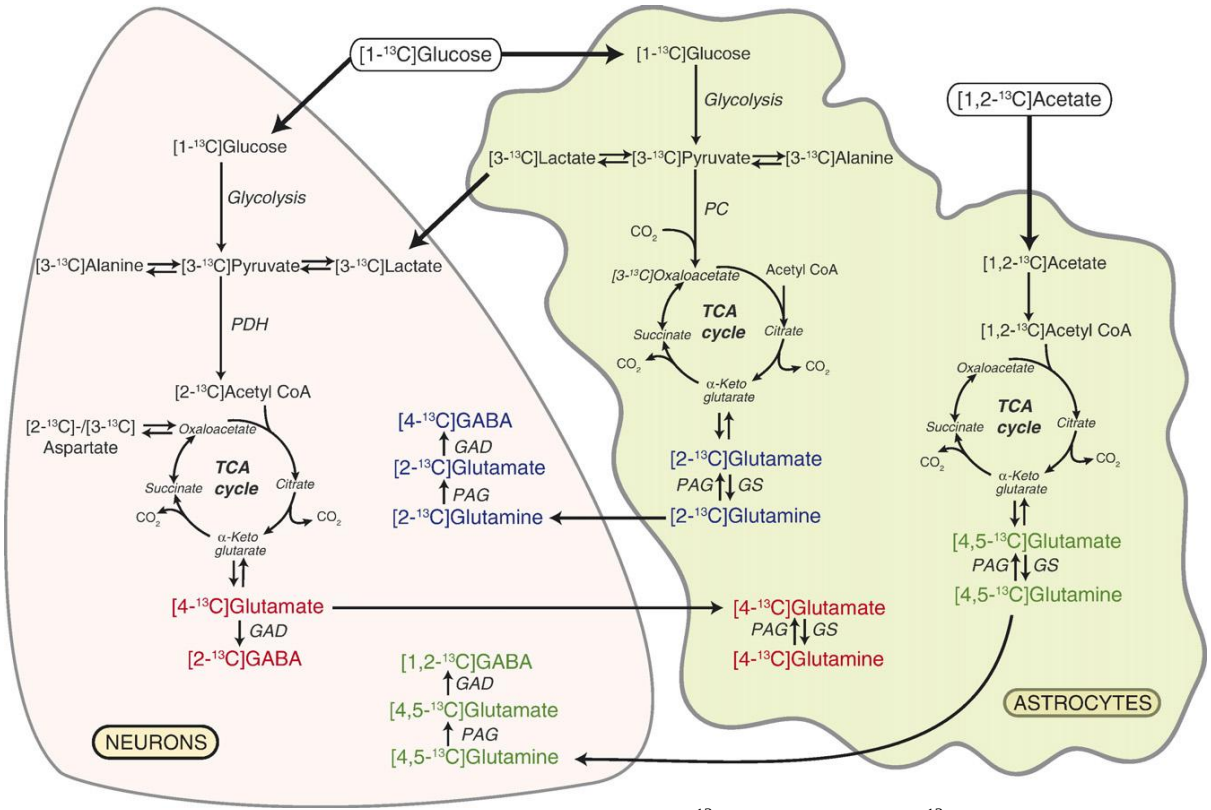

Figure 9. Labelling patterns derived from the metabolism of [1-[13]C]glucose and [1,2-[13]C]acetate in neurons and astrocytes, after glycolysis and one turn of the TCA-cycle. For a simplified diagram, the metabolite labelling yielded from the second turn of the TCA-cycle and the reaction with PDH in astrocytes are not shown. PDH = pyruvate dehydrogenase; PC = pyruvate carboxylase; PAG = phosphate-activated glutaminase; GS = glutamine synthetase; GAD = glutamic acid decarboxylase. Adapted from Melø et al. (2007).

3. Materials and methods

3.1 Conducted in Strasbourg, France

A total of 32 Adult male Sprague-Dawley rats (provided by Charles River Breeding Center, L'Arbresle, France) were given lithium chloride (3 meq/kg, i.p., Sigma, St Louis, Mo, U.S.A.) followed by methylscopolamine bromide ca. 20 hours later, in order to reduce the peripheral effects of pilocarpine. The rats were then divided into three groups:

1. The control group received only lithium chloride and vehicle.
2. The reference group received pilocarpine hydrochloride (25 mg/kg, s.c., Sigma) 30 min after methylscopolamine bromide. The induction of SE was confirmed when rats did not react to contact and experienced hypersalivation, usually after 3-4 stage IV-V seizures. Diazepam (2.5 mg/kg and 1.25 mg/kg) was then injected 1h and 9h post SE respectively in order to evaluate the effects of SE on epileptogenesis and neuronal death.
3. The treatment group received pilocarpine hydrochloride as the reference group, as well as an i.p. injection of 90 mg/kg carisbamate (CRS) in 45% hydroxypropyl-beta-cyclodextrin (Acros Organics, Geel, Belgium) 1h and 9h post SE. The rats received this CRS treatment (s.c.) twice daily for six more days. About 50% of these developed classical TLE whereas the remainders developed absence-like epilepsy with greater neuroprotection and response to treatment.

During SE, three rats died; two in the reference group and one in the treatment group. At 2 months after SE, the epileptic state of the animals was determined for the remaining 22 lithium-pilocarpine treated rats. [1-^{13}C]glucose and [1,2- ^{13}C]acetate was then injected i.p. 20 minutes before the rats were subjected to microwave fixation. The brains were removed and the hippocampus, piriform/entorhinal cortex, thalamus and amygdala were dissected, weighted and stored at -80°C until extraction.

All experiments were conducted in accordance with rules of the European Communities Council Directive of November 24, 1986 (86/609/EEC), the UK Animals (Scientific procedure) Act, 1986 and the French Department of Agriculture (License N° 67-97). The ethical Animal Research Committee Board of Louis Pasteur University (CREMEAS #AL/01/04/03/07) agreed to the experimentation protocol.

3.2 Conducted at NTNU, Trondheim

(*For this thesis, only the thalamic samples were analysed.)*

Tissue extraction

Methanol-chloroform double extractions were performed on all the samples in order to analyse the metabolites with HPLC and NMR spectroscopy. L-2-aminobutyric acid (α-ABA) was added to account for potential tissue loss during the extractions. This procedure is based on a method developed by Lindy Rae, revised by Mussie Ghezu, Lars Evje and Ursula Sonnewald to fit this experiment in particular. For full extraction procedure, see Appendix.

HPLC procedure

The equipment utilised was an Agilent 1200 HPLC consisting of a binary pump with degasser, autosampler, column oven (35°) and a fluorescence detector. The column was a Zorbax Eclipse XDB-C18 (eXtra Dense Bonding), 4.6x150 mm, 5 micron, Part no. 993967-902 (Agilent). The derivatisation agent used was o-phthaldialdehyde (OPA), and the excitation and emission wavelengths for the fluorescence detector were 230 and 450 nm respectively. Methanol and 10mM phosphate buffer (pH 7.1) was used as the mobile phase. A solvent gradient with increasing amounts of methanol was used. Standard solutions of different concentrations were used for the standard curves, and for every five samples a standard was run as a control. α-ABA was used as an internal standard to account for tissue loss during the extraction.

The extracted samples were lyophilised before they were dissolved in 200 µl of D_2O (deuterated water). 10 µl of each sample was then added to 90 µl of H_2O (1:10 dilution) in HPLC vials and run on the HPLC. The concentration of some of the metabolites was greater than that of the highest standard solution. Therefore, a further 1:10 dilution of the samples was necessary. The peaks were then integrated; however, only the glutamate, glutamine and GABA from the 1:100 dilution and aspartate from the 1:10 dilution were used for the statistical analysis.

NMR procedure

The remaining 190 µl which did not go to HPLC were lyophilised, redissolved in 200 µl of D_2O and lyophilised again to remove residual protons. 120µl of the standard, which was D_2O with 0.3g/L of TSP (2,2,3,3-tetradeutero-3-trimethylsilylpropionic acid) and 0.1% ethylene

glycol was then added before the samples were vortexed, centrifuged and put in SampleJet tubes (3.0x103.5mm).

A QCl CryoProbe^{TM} 600 MHz ultrashielded Plus magnet and a SampleJet autosampler (Bruker BioSpin GmbH, Reinstetten, Germany) were used to analyse the NMRS samples derived from [1-^{13}C]glucose and [1,2-^{13}C]acetate. For the ^{1}H spectra, a pulse angle of 90° was used, with a total number of 128 scans per sample. The acquisition time for each scan was 2.66 seconds, with a 10 second relaxation delay. For the ^{13}C spectra, the pulse angle was 30°, and the total number of scans was 10 000. The acquisition time was 1.65 seconds, with a relaxation delay of 0.5 seconds.

In order to determine and quantify the relevant peaks, the TopSpin^{TM} 3.0 software (Bruker BioSpin GmbH, Reinstetten, Germany) was used. For the ^{1}H spectra, it was necessary to do manual baseline correction, as well as phasing, for each peak. TSP was used as the standard with a known amount and set to 0.00 ppm. To get the concentration of the metabolites (in μmol/g), the area of the relevant peaks was corrected for the number of protons within the same chemical microenvironment, in addition to the sample weight, of which 95% was utilised for the NMRS procedure. Furthermore, tissue loss during the extraction was corrected for by using the α-ABA from the 1:10 diluted HPLC results.

For the ^{13}C spectra, the baseline was automatically corrected by the software. The relevant isotopomers were integrated, and their areas as well as the ethylene glycol peak at 63.7 ppm were used to calculate the concentrations (nmol/g). The differences in relaxation time and the nOe between ethylene glycol and the other peaks were corrected for, in addition to the sample weight and the tissue loss during extraction, the latter in the same manner as with the ^{1}H spectra.

The percent enrichment gives a good indication of the turnover, and in order to calculate this, the natural abundance had to be subtracted from the concentration of the isotopomer. If the isotopomer was mono-labelled, the following equation was used:

$$\frac{[^{13}\text{C-isotopomer}] - [\text{Total metabolite}]*0.011}{[\text{Total metabolite}]} \text{ x } 100$$

If the isotopomer was double-labelled, the equation was:

$$\frac{[^{13}\text{C-isotopomer}] - [\text{Total metabolite}]*0.011^{2}}{[\text{Total metabolite}]} \text{ x } 100$$

Calculations

In astrocytes, the first round of TCA cycling derived from PC activity generates [2-^{13}C]glutamate and thereafter [2-^{13}C]glutamine, or [4-^{13}C]GABA. However, these isotopomers are also generated from the second round of the TCA cycle derived from PDH activity. Additionally, the latter is produced from the second round of the TCA cycle derived from [1,2-^{13}C]acetate. In order to get the amounts for the PC contribution only, the amounts from PDH activity and [1,2-^{13}C]acetate need to be subtracted. For glutamate (glu) and glutamine (gln), the following equations were used:

$$[2\text{-}^{13}\text{C}]\text{glu/gln}-([3\text{-}^{13}\text{C}]\text{glu/gln}-[1,2\text{-}^{13}\text{C}]\text{glu/gln})$$

For [4-^{13}C]GABA, the equation is:

$$[4\text{-}^{13}\text{C}]\text{GABA}-[3\text{-}^{13}\text{C}]\text{GABA}$$

The ratio of metabolites produced during the second round of the TCA cycle over the first gives a good indication of the turnover and mitochondrial metabolism. For glutamate and glutamine derived from [1-^{13}C]glucose, this was calculated by using the following equation:

$$\frac{2\text{x}[3\text{-}^{13}\text{C}]\text{glu/gln}-[1,2\text{-}^{13}\text{C}]\text{glu/gln}}{[4\text{-}^{13}\text{C}]\text{glu/gln}}$$

This calculation was however not performed for GABA, as both [4-^{13}C]GABA and [3-^{13}C]GABA are generated from PDH and [1,2-^{13}C]acetate activity, and can thus not be distinguished from each other.

The turnover of [1,2-^{13}C]acetate was calculated by utilising the following equations:

$$\frac{2\text{x}[1,2\text{-}^{13}\text{C}]\text{glu/gln}}{[4,5\text{-}^{13}\text{C}]\text{glu/gln}}$$

Again, this calculation was not performed for GABA, for the same reason as for the [1-^{13}C]glucose turnover calculation for GABA.

The PC/PDH ratio gives an indication of the PC and PDH enzyme contribution for the entry of [1-^{13}C]glucose-derived metabolites into the TCA cycle. For glutamate/glutamine, the following equation was utilised:

$$\frac{[2\text{-}^{13}\text{C}]\text{glu/gln}-([3\text{-}^{13}\text{C}]\text{glu/gln}-[1,2\text{-}^{13}\text{C}]\text{glu/gln})}{[4\text{-}^{13}\text{C}]\text{glu/gln}}$$

The PC/PDH equation for GABA is:

$$\frac{([4\text{-}^{13}\text{C}]\text{GABA}-[3\text{-}^{13}\text{C}]\text{GABA})}{[2\text{-}^{13}\text{C}]\text{GABA}}$$

The [1,2-^{13}C]acetate contribution relative to the [1-^{13}C]glucose contribution for mitochondrial metabolism was then calculated. For glutamate and glutamine, the following equation was used:

$$\frac{[4,5\text{-}^{13}\text{C}]\text{glu/gln}}{[4\text{-}^{13}\text{C}]\text{glu/gln}}$$

For GABA, the equation is:

$$\frac{[1,2\text{-}^{13}\text{C}]\text{GABA}}{[2\text{-}^{13}\text{C}]\text{GABA}}$$

Finally, the transport of metabolites from astrocytes to glutamatergic and GABAergic neurons, as well as from neurons to astrocytes was calculated. The following equation was used for the transport from astrocytes to glutamatergic neurons:

$$\frac{[4,5\text{-}^{13}\text{C}]\text{glutamate}}{\%^{13}\text{C enrichment } [4,5\text{-}^{13}\text{C}]\text{glutamine}}$$

The equation utilised for the transport of metabolites from astrocytes to GABAergic neurons is:

$$\frac{[1,2\text{-}^{13}\text{C}]\text{GABA}}{\%^{13}\text{C enrichment } [4,5\text{-}^{13}\text{C}]\text{glutamine}}$$

The transport from neurons to astrocytes was calculated by using the following equation:

$$\frac{[4\text{-}^{13}\text{C}]\text{glutamine}}{\%^{13}\text{C enrichment } [4\text{-}^{13}\text{C}]\text{glutamate}}$$

Note: samples from five rats were not used in the ^{1}H-NMR analysis, and samples from two rats were not used in the ^{13}C-NMR analysis in this thesis. This was due to poor injection and sacrification.

Statistics

The results were analysed using One-Way ANOVA, where p-values below 0.05 were considered as statistically significant.

4. Results

Typical ^{1}H-NMR and ^{13}C-NMR spectra of the thalamic extracts of adult male rats are displayed in Figure 10 and Figure 11 respectively**.** Although more peaks were integrated, the labelled peaks are the ones used in the results for this thesis.

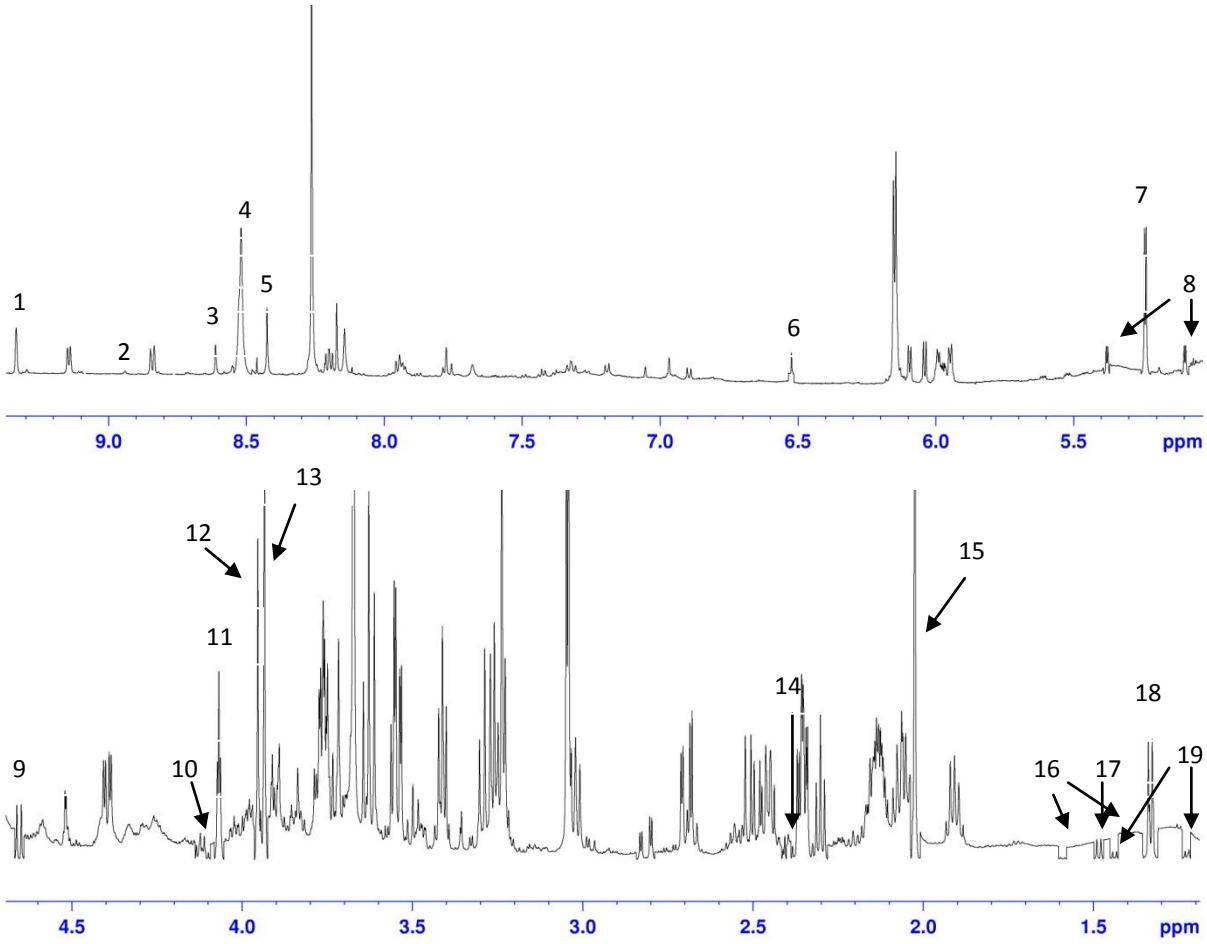

Figure 10. A typical ^{1}H-NMR spectrum. 1=NAD^{+}/$NADP^{+}$; 2=NADH/NADPH; 3=AMP; 4=ADP+ATP; 5=formate; 6=fumarate; 7=α-glucose; 8= α-glucose satellites; 9=β-glucose; 10=lactate; 11:myoinositol; 12=phosphocreatine; 13=creatine; 14=succinate; 15=N-acetyl aspartate (NAA); 16=alanine satellites; 17=alanine; 18=lactate; 19=lactate satellites; ppm=parts per million. Note: for a better view, the peaks from 5-9.4 ppm were made larger relative to the peaks from 1.2-4.7 ppm.

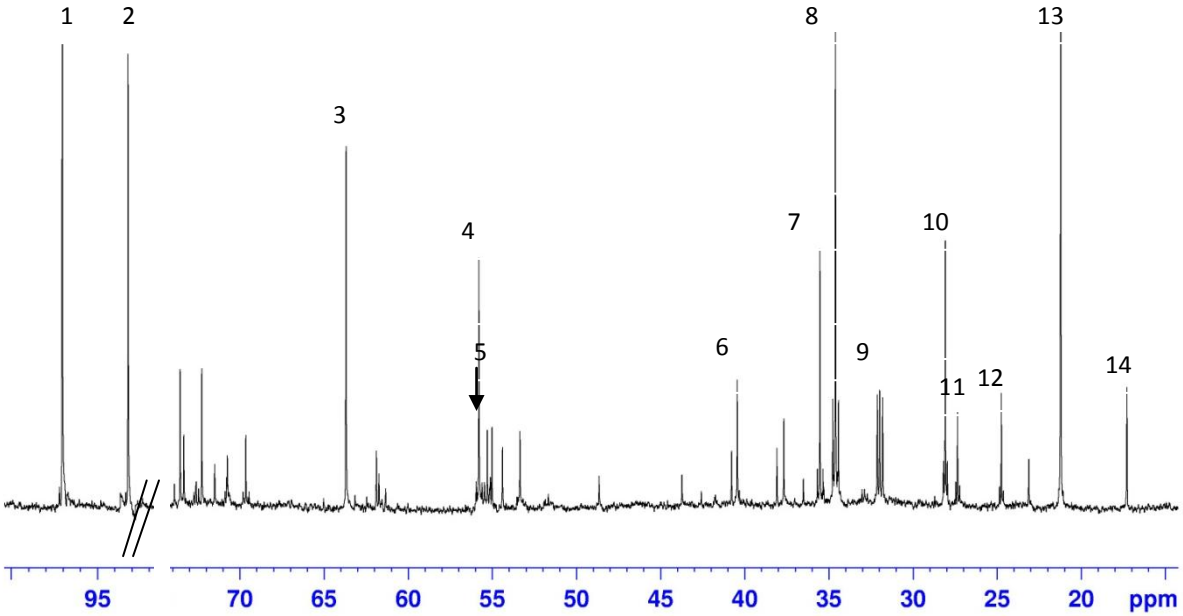

Figure 11. A typical ^{13}C-NMR spectrum. 1=β-glucose; 2=α-glucose; 3=ethylene glycol (reference peak); 4=glutamate C2; 5=glutamine C2; 6=GABA C4; 7=GABA C2 + succinate; 8=glutamate C4; 9=glutamine C4; 10=glutamate C3; 11=glutamine C3; 12=GABA C3;13=lactate C3; 14=alanine; ppm=parts per million.

4.1 Glycolytic activity

Adult male Sprague-Dawley rats were injected with [1-^{13}C]glucose and [1,2-^{13}C]acetate before being subjected to microwave fixation 20 minutes later. ^{1}H-NMR spectra were then taken of brain tissue extracts and used for the quantification of total thalamic glucose, lactate and alanine in the epilepsy group and the two treatment groups. Furthermore, the incorporation of ^{13}C label into metabolites was calculated using values from the glucose satellites in the ^{1}H-NMR spectra, corrected for the naturally abundant ^{13}C (1.1%), whereas the % ^{13}C enrichment was determined by dividing the total excess ^{13}C enrichment by the total concentration and multiplying with 100. For formulas, see Materials and Methods. Glycolytic activity is reflected by the incorporation of ^{13}C label into alanine and lactate, since pyruvate may be transaminated to the former, reduced to the latter, or oxidised to enter into the TCA-cycle. As seen in Table 1, there is a marked increase in both the total concentration and amount of ^{13}C enrichment of glucose for the TLE-group relative to the treatment groups, whereas the % ^{13}C enrichment remained the same for all. However, there is no change in the concentration of, and % ^{13}C enrichments with, lactate and alanine for the three groups compared to control.

Table 1. Total thalamic concentration (μmol/g wet weight), amount of ^{13}C label (μmol/g) and % ^{13}C enrichment with glucose, lactate and alanine in adult rats injected with [1-^{13}C]glucose and [1,2-^{13}C]acetate.

	Control N=6	TLE N=4	CRS-TLE N=9	CRS-ALE N=5
Total glucose	3.8±0.8	6.5±0.6[a]	3.8±0.5[b]	3.3±0.4[b]
Total ^{13}C	1.2±0.2	1.9±0.2[a]	1.1±0.1[b]	1.0±0.1[b]
% ^{13}C enrichment	27.4±3.3	29.6±1.5	28.1±2.1	31.3±2.4
Total lactate	8.7±3.2	7.3±2.9	8.2±3.3	3.1±0.2
Total ^{13}C	1.0±0.4	0.7±0.3	0.9±0.3	0.3±0.05
% ^{13}C enrichment	11.6±0.7	8.2±1.0	10.4±1.1	10.4±1.4
Total alanine	0.9±0.2	1.1±0.3	0.6±0.1	0.5±0.1
Total ^{13}C	0.1±0.02	0.1±0.03	0.1±0.02	0.1±0.002
% ^{13}C enrichment	11.8±0.5	9.2±0.9	11.1±0.8	12.3±1.4

Adult rats were injected with [1-^{13}C]glucose and [1,2-^{13}C]acetate before being subjected to microwave fixation 20 minutes later. The thalamus extracts were analysed using ^{1}H-NMR and ^{13}C-NMR spectroscopy. For more details, see Materials and Methods. Values are mean±SEM. TLE = untreated temporal lobe epilepsy; CRS-TLE = carisbamate-treated temporal lobe epilepsy, and CRS-ALE = carisbamate-treated absence-like epilepsy. [a] and [b] signify statistical significance relative to the control and TLE respectively ($p<0.05$).

4.2. Total metabolite amounts

The total concentration of glutamate, glutamine, γ-aminobutyric acid (GABA), and aspartate was quantified using HPLC. Figure 12 shows that glutamate content was decreased for the TLE group compared to the control, CRS-TLE and CRS-ALE groups, whereas that in the CRS-TLE group was decreased relative to the control. For the glutamine content, the TLE group had a decreased concentration only compared to the CRS-ALE group, whereas the levels of GABA were increased in the control and CRS-TLE groups relative to the TLE and CRS-ALE groups. The levels of aspartate were higher in the control compared to the other three groups, as well as in the CRS-ALE group compared to the TLE group.

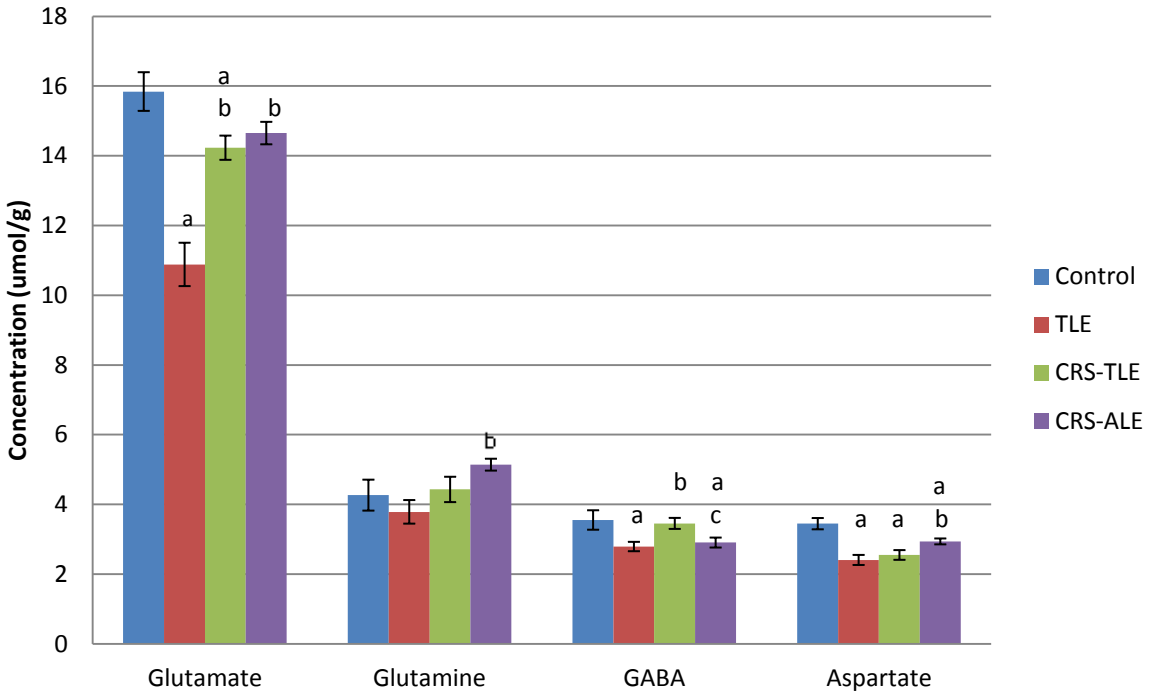

Figure 12. Total concentration (µmol/g wet weight) of glutamate, glutamine, GABA and aspartate. The thalamus extracts were analysed using HPLC. For more details, see Materials and Methods. Values are mean±SEM. TLE = untreated temporal lobe epilepsy; CRS-TLE = carisbamate-treated temporal lobe epilepsy, and CRS-ALE = carisbamate-treated absence-like epilepsy. [a],[b] and [c] signify statistical significance relative to the control, TLE and CRS-TLE respectively ($p<0.05$). N=7(CTRL), 4(TLE), 11(CRS-TLE) and 7(CRS-ALE); except for glutamate which has N=10 (CRS-TLE).

The concentration (µmol/g wet weight) of a range of metabolites was also quantified using ^{1}H-NMR spectra. From Table 2 it is clear that the only metabolites showing a difference between the groups are formate and N-acetylaspartate (NAA). For formate, there was an increase in the CRS-TLE group relative to the control. NAA, on the other hand, showed a decrease in the TLE group compared to the other three groups, and also in the CRS-TLE group compared to the control.

Table 2. Total concentration (μmol/g wet weight) of thalamic metabolites taken from the ^{1}H-NMR spectra.

Metabolite	CTRL N=6	TLE N=4	CRS-TLE N=9	CRS-ALE N=5
$NAD^+/NADP^+$	0.2±0.1	0.1±0.1	0.3±0.1	0.3±0.1
NADH/NADPH	0.4±0.1	0.3±0.1	0.1±0.1	0.1±0.1
Adenosine ph.	0.9±0.6	0.6±0.6	1.7±0.4	1.9±0.6
Formate	0.06±0.007	0.07±0.007	0.086±0.007[a]	0.07±0.009
Fumarate	0.1±0.02	0.1±0.02	0.1±0.02	0.04±0.002
Myoinositol	9.5±0.4	8.9±0.5	9.3±0.3	8.6±0.3
Phosphocreatine	1.1±0.6	1.0±0.6	1.9±0.5	2.4±0.3
Creatine	6.9±0.5	6.0±0.8	5.8±0.6	5.2±0.1
Taurine	3.8±0.3	3.9±0.5	4.4±0.2	3.9±0.2
Succinate	0.1±0.01	0.1±0.01	0.2±0.1	0.1±0.01
NAA	8.2±0.4	6.0±0.4[a]	7.2±0.2[ab]	7.6±0.3[b]

Total concentration is given in μmol/g wet weight. The thalamus extracts were analysed using ^{1}H-NMRS. For more details, see Materials and Methods. Values show mean±SEM. CTRL= control; TLE = untreated temporal lobe epilepsy; CRS-TLE = carisbamate-treated temporal lobe epilepsy, and CRS-ALE = carisbamate-treated absence-like epilepsy; NAD(P)+ = nicotinamide adenine dinucleotide (phosphate), oxidised form; NADH(P) = nicotinamide adenine dinucleotide (phosphate), reduced form; adenosine ph. = adenosine mono-, di- and triphosphate; NAA = N-acetylaspartate. [a] and [b] signify statistical significance relative to the control and TLE respectively ($p<0.05$).

4.3. Isotopomer amounts

In order to get a better look at the neuronal and astrocytic metabolism of the thalamus, ^{13}C-NMR spectra were used to determine the concentration of ^{13}C labeled isotopomers derived from [1-^{13}C]glucose and [1,2-^{13}C]acetate. This was done by subtracting the natural abundance of ^{13}C isotopes; the calculation can be seen in Materials and Methods. The isotopomers derived from [1-^{13}C]glucose only, include [4-^{13}C]glutamate and [4-^{13}C]glutamine, which are produced during the first turn of the TCA cycle. Both of these showed a decreased amount in the TLE group relative to the control (Table 3). This result was also obtained for [2-^{13}C]glutamate, which is produced during the second turn of the TCA cycle, as well as from pyruvate carboxylation (PC). Furthermore, [3-^{13}C]glutamate and [4-^{13}C]GABA, which are produced from the second turn of both [1-^{13}C]glucose and [1,2-^{13}C]acetate derived TCA cycle activity, showed a reduction in the TLE and CRS-ALE groups relative to the control respectively.

The isotopomers derived from [1,2-^{13}C]acetate produced in the first round of the TCA cycle, [4,5-^{13}C]glutamate and [1,2-^{13}C]GABA, were both reduced in the TLE, CRS-TLE and CRS-ALE groups relative to the control. Furthermore, the concentration of [1,2-^{13}C]glutamate, which is produced in the second turn of the TCA cycle, showed a reduction in

both the CRS-TLE and CRS-ALE groups relative to the control. There concentration of [4,5-^{13}C]- and [1,2-^{13}C]glutamine, however, remained unaltered between the groups.

Pyruvate may be oxidised to acetyl-CoA via the pyruvate dehydrogenase complex (PDH) for mitochondrial metabolism. However, it may also enter the TCA cycle via PC for anaplerotic reactions in astrocytes. This accounts for 10% of the total glucose metabolism (104). In order to find out whether the balance between PC and PDH activity was altered, the concentration of metabolites derived from PC activity was determined. The first round of TCA cycle activity derived from PC generates [2-^{13}C]glutamate and thereafter [2-^{13}C]glutamine, and [4-^{13}C]GABA. Nonetheless, these isotopomers are also derived from PDH activity, and the latter also from [1,2-^{13}C]acetate. Calculations are therefore required to get amounts from PC contribution only. Formulas can be seen in Materials and Methods. As seen in Table 3, the PC activity, displayed with an *, was only altered between the groups for GABA, as the TLE, CRS-TLE and CRS-ALE groups had decreased levels compared to the control.

Table 3. Amount of ^{13}C-labelled isotopomers (nmol/g wet weight) of thalamic glutamate, glutamine and GABA derived from [1-^{13}C]glucose and [1,2-^{13}C]acetate, as well as amount of metabolites derived from pyruvate carboxylation.

Precursor	Isotopomer	CTRL N=6	TLE N=4	CRS-TLE N=11	CRS-ALE N=6
[1-^{13}C]glucose	[4-^{13}C]glutamate	744.9±57.1	463.0±70.8[a]	615.8±49.7	598.3±51.1
	[2-^{13}C]glutamate	234.9±27.0	119.3±34.0[a]	184.4±29.6	161.9±22.9
	[2-^{13}C]glutamate*	98.7±17.6	58.4±15.8	64.9±9.4	61.7±8.6
	[4-^{13}C]glutamine	151.4±19.5	98.7±18.5[a]	129.8±10.9	147.7±14.8
	[2-^{13}C]glutamine	82.9±13.1	67.0±11.0	75.8±8.5	78.0±10.2
	[2-^{13}C]glutamine*	63.6±18.2	64.6±12.2	52.9±7.4	41.0±11.0
	[2-^{13}C]GABA	162.2±34.3	92.0±29.4	127.2±24.5	83.1±8.8
Both	[3-^{13}C]glutamate	181.2±16.6	89.1±24.2[a]	142.1±26.7	122.1±17.8
	[3-^{13}C]glutamine	75.9±12.0	57.6±9.9	61.7±4.7	70.7±7.7
	[3-^{13}C]GABA	32.7±11.2	14.3±7.0	24.1±10.9	10.2±3.4
	[4-^{13}C]GABA	59.7±15.7	23.8±11.1	37.4±13.0	14.9±4.4[a]
	[4-^{13}C]GABA*	27.1±7.0	9.4±4.2[a]	14.0±3.1[a]	5.9±1.9[a]
[1,2-^{13}C]acetate	[1,2-^{13}C]glutamate	45.0±5.8	28.2±6.2	22.7±4.6[a]	22.0±5.0[a]
	[4,5-^{13}C]glutamate	172.2±25.5	109.0±20.1[a]	112.1±12.2[a]	111.1±9.8[a]
	[1,2-^{13}C]glutamine	56.6±13.2	55.2±9.1	38.9±8.4	33.7±8.7
	[4,5-^{13}C]glutamine	255.8±26.6	197.5±48.3	188.5±24.4	237.7±24.9
	[1,2-^{13}C]GABA	48.3±9.8	20.0±8.1[a]	23.4±5.2[a]	17.6±5.7[a]

Adult rats were injected with [1-^{13}C]glucose and [1,2-^{13}C]acetate before being subjected to microwave fixation 20 minutes after. The thalamus extracts were analysed using ^{13}C-NMR spectroscopy, and values are shown in nmol/g wet weight. Values are mean±SEM. TLE = untreated temporal lobe epilepsy; CRS-TLE = carisbamate-treated temporal lobe epilepsy, and CRS-ALE = carisbamate-treated absence-like epilepsy. * = Isotopomers derived from PC contribution. [a] denotes statistical significance relative to the control ($p<0.05$).

4.4 The % 13C enrichments with isotopomers

The % ^{13}C enrichments (Table 4) were calculated using the concentration of isotopomers corrected for natural abundance (Table 3), divided by the total metabolite concentration, determined by HPLC, and multiplying by 100. For formula, see Materials and Methods. For the isotopomers derived from [1-^{13}C]glucose, only [2-^{13}C]glutamine showed a difference, with a decreased % ^{13}C enrichment in the CRS-ALE group relative to the control. Furthermore, only [4-^{13}C]GABA of the isotopomers derived from both [1-^{13}C]glucose and [1,2-^{13}C]acetate showed a decrease in the % ^{13}C enrichment, in both the CRS-TLE and CRS-ALE groups compared to the control. However, there were a lot more differences in the isotopomers derived from [1,2-^{13}C]acetate: [1,2-^{13}C]glutamate, [4,5-^{13}C]glutamate and [1,2-^{13}C]GABA all had a decreased % ^{13}C enrichment in the CRS-TLE and CRS-ALE groups relative to the control, whereas the former also had a decrease in the CRS-TLE group compared to the TLE group. Additionally, the % [1,2-^{13}C]- and [4,5-^{13}C]glutamine had decreased in the CRS-ALE and CRS-TLE groups relative to the control, respectively.

Table 4. % Enrichment with ^{13}C-labelled isotopomers of thalamic glutamate, glutamine and GABA derived from [1-^{13}C]glucose and [1,2-^{13}C]acetate.

Precursor	Isotopomer	CTRL N=6	TLE N=4	CRS-TLE N=11	CRS-ALE N=6
[1-^{13}C]glucose	[4-^{13}C]glutamate	4.6±0.3	4.2±0.5	4.1±0.3	4.0±0.3
	[2-^{13}C]glutamate	1.5±0.2	1.1±0.3	1.1±0.1	1.1±0.1
	[4-^{13}C]glutamine	3.7±0.4	2.6±0.5	2.9±0.2	2.9±0.2
	[2-^{13}C]glutamine	2.1±0.3	1.8±0.3	1.7±0.2	1.1±0.2[a]
	[2-^{13}C]GABA	4.4±0.6	3.2±1.0	3.2±0.5	3.0±0.4
Both	[3-^{13}C]glutamate	1.1±0.1	0.8±0.2	0.8±0.1	0.8±0.1
	[3-^{13}C]glutamine	1.8±0.2	1.5±0.2	1.4±0.1	1.4±0.1
	[3-^{13}C]GABA	0.9±0.2	0.5±0.2	0.4±0.1	0.4±0.1
	[4-^{13}C]GABA	1.6±0.3	0.8±0.4	0.8±0.2[a]	0.5±0.2[a]
[1,2-^{13}C]acetate	[1,2-^{13}C]glutamate	0.3±0.04	0.3±0.04	0.1±0.03[ab]	0.1±0.03[a]
	[4,5-^{13}C]glutamate	1.1±0.1	1.0±0.1	0.7±0.1[a]	0.8±0.1[a]
	[1,2-^{13}C]glutamine	1.4±0.3	1.4±0.1	0.9±0.2	0.6±0.2[a]
	[4,5-^{13}C]glutamine	6.3±0.6	5.1±0.9	4.3±0.5[a]	4.6±0.5
	[1,2-^{13}C]GABA	1.3±0.2	0.7±0.3	0.6±0.1[a]	0.6±0.2[a]

Adult rats were injected with [1-^{13}C]glucose and [1,2-^{13}C]acetate before being subjected to microwave fixation 20 minutes after. The % enrichments were calculated using values from ^{13}C-NMRS and HPLC. For more details, see Materials and Methods. Values show mean±SEM. TLE = untreated temporal lobe epilepsy; CRS-TLE = carisbamate-treated temporal lobe epilepsy, and CRS-ALE = carisbamate-treated absence-like epilepsy. [a] and [b] denote statistical significance relative to the control and TLE respectively ($p<0.05$).

4.5 Ratios

The ratio of metabolites produced during the second round of the TCA cycle over the first gives a good indication of the turnover of mitochondrial metabolism. For formulas, see Materials and Methods. As seen in Table 5, there was no change in the metabolic turnover between the groups for the [1-^{13}C]glucose derived glutamate and glutamine. Furthermore, apart from a decreased turnover in the CRS-ALE group relative to the TLE group in glutamine, there was no change in the metabolic rates for [1,2-^{13}C]acetate derived metabolites.

In addition to the amounts of PC derived metabolites (Table 3), the ratio of PC over PDH was calculated to see if there were any changes in the ratio of [1-^{13}C]glucose derived metabolites destined for anabolism and catabolism. As seen in Table 5, only the CRS-ALE group showed a decrease relative to the TLE group for glutamine and the control group for GABA. The ratio of [1,2-^{13}C]acetate over [1-^{13}C]glucose consumption was then calculated in order to see if there was a difference in the preferred energy substrate between the groups. This was done by dividing the amount of isotopomer derived from [1,2-^{13}C]acetate with the amount from [1-^{13}C]glucose, both from the first round of the TCA cycle and the latter via the PDH complex. See Materials and Methods for the formula. There was no change in this ratio, apart from for GABA, which had a reduction in the CRS-TLE group compared to the control.

The transport of [1,2-^{13}C]acetate derived metabolites from astrocytes to glutamatergic neurons was also calculated, by dividing the amount of [4,5-^{13}C]glutamate by the % ^{13}C enrichment with [4,5-^{13}C]glutamine. Furthermore, the transport from astrocytes to GABAergic neurons was calculated by dividing the amount of [1,2-^{13}C]GABA by the % ^{13}C enrichment with [4,5-^{13}C]glutamine. For both types of neurons there was no change in the transport from astrocytes, except for a decreased transport to the GABAergic neurons in the CRS-ALE group relative to the control (Table 5). The neuron to astrocyte transport was also calculated, by dividing the amount of [4-^{13}C]glutamine by the % ^{13}C enrichment with [4-^{13}C]glutamate. In this case there was a marked decrease in the TLE group relative to the other three.

Table 5. Ratios

		CTRL N=6	TLE N=4	CRS-TLE N=11	CRS-ALE N=6
Glucose $2^{nd}/1^{st}$	Glutamate	0.4±0.02	0.3±0.1	0.4±0.05	0.4±0.03
	Glutamine	0.6±0.1	0.6±0.1	0.6±0.1	0.7±0.1
Acetate $2^{nd}/1^{st}$	Glutamate	0.5±0.04	0.5±0.1	0.4±0.1	0.4±0.1
	Glutamine	0.4±0.1	0.6±0.1	0.4±0.1	0.4±0.1[b]
PC/PDH	Glutamate	0.1±0.02	0.1±0.02	0.1±0.01	0.1±0.01
	Glutamine	0.4±0.1	0.7±0.1	0.4±0.1	0.3±0.1[b]
	GABA	0.2±0.03	0.1±0.03	0.1±0.03	0.06±0.03[a]
Acetate/glucose	Glutamate	0.2±0.03	0.2±0.01	0.2±0.02	0.2±0.02
	Glutamine	1.7±0.2	2.0±0.3	1.6±0.3	1.6±0.1
	GABA	0.3±0.02	0.22±0.1	0.18±0.1[a]	0.21±0.1
From astrocytes	To glutamatergic	27.6±3.8	22.0±3.0	25.3±2.2	24.2±0.5
	To GABAergic	7.8±1.7	3.6±1.6	4.9±1.2	3.6±0.9[a]
From neurons	To astrocyte	32.7±3.7	22.8±2.2[a]	32.6±1.6[b]	36.5±1.8[b]

Adult rats were injected with [1-^{13}C]glucose and [1,2-^{13}C]acetate before being subjected to microwave fixation 20 minutes after. The thalamus extracts were analysed using ^{13}C-NMRS. For more details, see Materials and Methods. Values show mean±SEM. TLE = untreated temporal lobe epilepsy; CRS-TLE = carisbamate-treated temporal lobe epilepsy, and CRS-ALE = carisbamate-treated absence-like epilepsy; PC = pyruvate carboxylase; PDH = pyruvate dehydrogenase. [a] and [b] denote statistical significance relative to the control and TLE group respectively ($p<0.05$).

5. Discussion

The rats used in the experiments described in the thesis were initially divided into three groups. One was the control group, consisting of seven animals, which received saline injection and thus did not develop epilepsy. The second group was the untreated TLE group, initially consisting of six rats (four survived) which received lithium-chloride and pilocarpine, followed by a small injection of diazepam in order to stop the status epilepticus. The third group was the carisbamate treated group, initially consisting of 19 animals (one died) which received carisbamate following the lithium-chloride and pilocarpine injections. This group was then later divided into two based on whether they developed TLE (CRS-TLE) or absence-like epilepsy (CRS-ALE). For this thesis I have chosen to show most of the results obtained from the experiments; however, since this is a masters degree thesis I will only focus on the major findings in the discussion. Furthermore, since the TLE group contained only four animals, the results often showed large variances that made it difficult to reach statistical significance. This was also kept in mind when writing the discussion.

5.1 Glycolytic activity in untreated TLE

After glucose enters the cell, glycolysis is the first part of its metabolism, and if the substrate is one mole of [1-^{13}C]glucose, the yield will be one mole of [3-^{13}C]pyruvate and one mole of unlabelled pyruvate. In the following I will only describe the fate of the labelled metabolites since no excess ^{13}C label is present in the unlabelled compounds. [3-^{13}C]pyruvate may either be transaminated to become [3-^{13}C]alanine, be reduced to [3-^{13}C]lactate or oxidised to [2-^{13}C]acetyl-CoA for the entry into the TCA cycle. The untreated TLE group showed a lower glucose consumption compared to the control, as the concentration of both total glucose and ^{13}C label were higher, and the % ^{13}C enrichment remained the same (Table 1). This is in accordance with several studies, both in animals and humans, that have demonstrated interictal hypometabolism in the chronic phase of TLE (105,106). Moreover, as there was no change in the concentration of alanine and lactate in this study (Table 1), it appears that there was less glucose entering the TCA cycle in the TLE group relative to the other groups.

5.2 Neuronal and astrocytic TCA cycle activity in untreated TLE

5.2.1 Reduced TCA cycle activity

Indications of reduced TCA cycle activity can be seen when looking at the total concentration of glutamate, GABA and aspartate (Figure 12) which was lower in the TLE group relative to the control, thus corresponding well with the results regarding the glucose consumption (Table 1). There was, however, no significant difference for glutamine in the TLE group relative to the control. This is in agreement with a study performed by Melø et al. (107), in which there was also no difference between the glutamine levels in the control and epileptic rats. As glutamine is synthesised in astrocytes from glutamate via GS, this could indicate that astrocytic metabolism in the thalamus is unaffected by TLE, as opposed to the neuronal metabolism. However, it has previously been shown that astrogliosis occurs in the pilocarpine rat model, though with large variations both between animals and different brain regions within animals (108). Furthermore, the activity of GS has been shown to be reduced in reactive astrocytes (109). Therefore, the similar levels of glutamine in the TLE and control groups could also reflect this.

The concentration of several metabolites obtained from ^{1}H-NMRS has been displayed (Table 2), although very little change was observed between the groups. Nevertheless, the metabolite worth mentioning is NAA, which showed a lower concentration in the TLE group compared to the control. Moreover, the levels of a AMP, ADP and ATP, here combined and referred to as adenosinephosphate, also showed a similar trend. The latter did however not reach statistical significance, which is likely due to the large SEM value caused by several NMR spectra with non-integratable peaks. Nonetheless, a lower level of both NAA and the adenosine phosphates signifies either neuronal death or a mitochondrial deficiency, and has previously been shown in different rat models of epilepsy (68,107).

5.2.2. [1-^{13}C]Glucose utilisation

By looking at the amounts of ^{13}C labelling for the different isotopomers of glutamate, glutamine and GABA, taken from ^{13}C-NMR spectra, it is possible to get a better understanding of the contribution of different metabolic pathways. In terms of neuronal mitochondrial metabolism, the entry of glucose-derived [3-^{13}C]pyruvate into the TCA cycle

occurs via the PDH enzyme. If [3-^{13}C]pyruvate is oxidised to [2-^{13}C]acetyl-CoA via PDH, the first round of the TCA cycle will produce [4-^{13}C]glutamate and subsequently [4-^{13}C]glutamine or [2-^{13}C]GABA. In this study, the amounts of both [4-^{13}C]glutamate and [4-^{13}C]glutamine were reduced in the TLE group relative to the control. The lower concentration of [4-^{13}C]glutamate corresponds well with the HPLC and ^{1}H-NMRS results, and is yet another indication of reduced mitochondrial TCA cycle activity. As mentioned above, the total amount of glutamine in the TLE group was not significantly different from the control. Therefore, it can be assumed that the decrease in [4-^{13}C]glutamine in the TLE group may be a result of an altered production of neuron-derived glutamate. It is however important to keep in mind that approximately 60% of the [4-^{13}C]glutamine is derived from the astrocytic PDH (110). Thus the lower amounts of [4-^{13}C]glutamine may also in part be due to a loss of GS and/or reduced GS activity, which has previously been demonstrated by Eid et al. in the hippocampal formation of MTLE patients (109). The ratio of transfer from neurons to astrocytes, which is calculated by dividing the concentration of [4-^{13}C]glutamine by the % ^{13}C enrichment with [4-^{13}C]glutamate, was also lower in the TLE group relative to the control. This makes sense since there was a lower concentration of [4-^{13}C]glutamine and the % ^{13}C enrichment with [4-^{13}C]glutamate was unchanged. In terms of [2-^{13}C]GABA, there was no significant difference between the TLE group relative to the control. However, as the difference between the amounts in the two groups is larger than between the two groups for [4-^{13}C]glutamine, it is clear that the lack of significance is due to large SEM values. It may therefore appear that the TLE group for [2-^{13}C]GABA was lower relative to the control, like with the two other isotopomers.

If the [2-^{13}C]- or [3-^{13}C]OAA from the first round of the TCA cycle enters the second round by condensing with unlabelled acetyl-CoA, then [2-^{13}C]- or [3-^{13}C]glutamate and thereafter glutamine, or [3-^{13}C]- or [4-^{13}C]GABA will be produced. OAA may also condense with labelled acetyl-CoA, though these results are not shown. However, the production of [2-^{13}C]glutamate, [2-^{13}C]glutamine and [4-^{13}C]GABA also occurs via the astrocytic enzyme PC, which contributes to 10% of the total glucose metabolism (104). The results have therefore been presented as the total concentrations of these isotopomers, in addition to the concentrations derived from PC contribution only. The concentration of total [2-^{13}C]glutamate was lower in the TLE group compared to the control, which is in line with the result that the turnover of glucose-derived glutamate between the two groups did not change. Furthermore, the levels of [2-^{13}C]glutamate derived from PC only were not significantly decreased in the

TLE group relative to the control. There was a slight reduction, however, which again might be due to an altered neuronal production of [2-^{13}C]glutamate from [2-^{13}C]glutamine rather than a metabolic dysfunction in the astrocytes. Another indication of this is that PC-derived [2-^{13}C]glutamine accounted for almost all of the [2-^{13}C]glutamine for the TLE group, but not the control, and the amounts were unchanged between the two groups. This indicates that the lower amount of [2-^{13}C]glutamine in the TLE group is due to a decrease in PDH activity. Surprisingly, however, the total amount of [4-^{13}C]GABA was not significantly reduced in the TLE group compared to the control, whereas the PC-derived [4-^{13}C]GABA was. Nevertheless, the fact that the latter also contained [4-^{13}C]GABA derived from [1,2-^{13}C]acetate, and that it is not possible to distinguish between the two, makes these results more uncertain.

5.2.3. [1,2-^{13}C]Acetate utilisation

As mentioned, PC contributes to approximately 10% of the glucose metabolism, and occurs only in astrocytes, which is also the place for 27% of the total PDH activity (26). Furthermore, astrocytes selectively take up acetate for its metabolism in the TCA cycle. In the present study, [1,2-^{13}C]acetate was injected, entered the astrocytes and was subsequently converted to [1,2-^{13}C]acetyl-CoA. In this first round of the TCA cycle, this labelling pattern produces [4,5-^{13}C]glutamate, and subsequently [4,5-^{13}C]glutamine, and [1,2-^{13}C]GABA. Even though astrocytic glutamine is generated from astrocytic glutamate, most of the glutamate in the brain resides within the neurons (111). Therefore, the [4,5-^{13}C]glutamate seen in this study is mainly a result of the transport of [4,5-^{13}C]glutamine into neurons and subsequent conversion into [4,5-^{13}C]glutamate. The concentration of [4,5-^{13}C]glutamine was unchanged in the TLE group relative to the control, whereas both [4,5-^{13}C]glutamate and [1,2-^{13}C]GABA were lower. The fact that the amounts were only slightly lower in [4,5-^{13}C]glutamine and significantly lower in the two other isotopomers is another indication of a fairly unaltered astrocytic metabolism. Nevertheless, the transfer from astrocytes to neurons, calculated by dividing [4,5-^{13}C]glutamate or [1,2-^{13}C]GABA by the % ^{13}C enrichment with [4,5-^{13}C]glutamine, was not significantly reduced in the TLE group compared to the control. The transport into glutamatergic neurons was however slightly reduced, whereas that into GABAergic neurons was more than halved but did not reach significance due to large SEM values.

If the label from [1,2-^{13}C]acetate remains in the TCA cycle for the second turn, it will yield [3-^{13}C]- or [1,2-^{13}C]glutamate, and subsequently glutamine, or [3-^{13}C]- or [4-^{13}C]GABA. The concentration of [1,2-^{13}C]glutamate was lower in the TLE group, though not significantly, whereas there was no change for [1,2-^{13}C]glutamine (Table 3). This is in line with the results that there was no change in the acetate turnover, which was calculated by doubling the amount of [3-^{13}C]glutamate/glutamine and dividing it by [4,5-^{13}C]glutamate/glutamine (Table 5). Since [3-^{13}C]- and [4-^{13}C]GABA are also generated during the second turn of PDH-derived TCA cycle activity, it is not possible to distinguish between these and the similarly labelled GABA derived from [1,2-^{13}C]acetate. Thus, it is also not possible to make a correct calculation of the TCA cycle turnover of [1,2-^{13}C]acetate-derived label for this metabolite.

In order to determine the contribution of acetate relative to glucose for the production of metabolites, this ratio was calculated for glutamate, glutamine and GABA. For the former two, this is done by dividing [4,5-^{13}C]glutamate/glutamine by [4-^{13}C]glutamate/glutamine. For glutamate there was no change in this ratio between the two groups (Table 5), as both isotopomers were reduced in the TLE group. The ratio for GABA, which was calculated by dividing [1,2-^{13}C]GABA with [2-^{13}C]GABA, did also not change significantly. Again, this could potentially be due to impaired neuronal rather than astrocytic metabolism. In this scenario, the acetate/glucose ratio for glutamine should show an increase in the TLE group relative to the control. However, this increase was only slight and did not reach significance, even though the concentrations of [4-^{13}C]glutamine and [4,5-^{13}C]glutamine were significantly lower and unchanged, respectively.

5.3. The effect of CRS on the neuronal and astrocytic metabolism in TLE

The animals receiving CRS developed either TLE (CRS-TLE) or absence-like epilepsy (CRS-ALE). The amounts of total glucose and ^{13}C label were lower in both the CRS-TLE and CRS-ALE groups compared to the untreated TLE group (Table 1), which indicates that the glucose consumption was not disturbed in these groups. The CRS-treated rats also showed a higher level of NAA compared to the TLE group (Table 2), thereby signifying that CRS either reduced cell death or restored the mitochondrial metabolism. Furthermore, there was a higher level of total glutamate (Figure 12) as well as glutamate derived from [1-^{13}C]glucose in the CRS-TLE and CRS-ALE groups (Table 3). It is worth noting, however, that the levels of [4,5-^{13}C]glutamate and [1,2-^{13}C]GABA were not increased relative to the control when CRS was

introduced, indicating that there was a decreased conversion of [4,5-^{13}C]glutamine into the two isotopomers relative to the control group (Table 3). This also resulted in a lower % ^{13}C enrichment with [4,5-^{13}C]glutamate and [1,2-^{13}C]GABA (Table 4).

The results from glutamine give another indication of unchanged mitochondrial metabolism in neurons. This is because the amounts of total glutamine were higher in the CRS-ALE and CRS-TLE groups relative to the TLE group (Figure 12), although the latter was not significant. Furthermore, the only glutamine isotopomers that showed a change relative to the TLE group were the ones derived from [1-^{13}C]glucose (Table 3). Thus astrocytes appear to be relatively unaffected by both temporal lobe epilepsy as well as the CRS treatment.This metabolic balance between the two cell types is also reflected by the decreased PC/PDH ratio for glutamine in the CRS-ALE group relative to the TLE group (Table 5). With GABA, however, it was the CRS-TLE group that showed unchanged levels relative to the control, whereas the CRS-ALE group remained equal to the TLE group (Figure 12). In terms of the GABA isotopomers, the thalamic amounts in the CRS-ALE group were consistently lower compared to CRS-TLE, although this was not significant (Table 3). There was also less transfer of GABA from astrocytes to GABAergic neurons in the CRS-ALE group compared to the control (Table 5).

5.4. Thalamic metabolic differences of TLE treated and ALE treated rats

In the present study, CRS has shown to improve the neuronal mitochondrial metabolism in rats of the lithium-pilocarpine model. However, it is of interest to see how the metabolism of the rats in the CRS-TLE and CRS-ALE groups is different. François et al (76) reported greater neuroprotection in thalamic nuclei of the CRS-ALE group relative to the CRS-TLE group. In terms of metabolism, however, the two groups are relatively similar. In fact, the only marked difference was the total concentration of GABA obtained from HPLC (Figure 12) The reason for why the amounts of GABA in the CRS-ALE group are lower than in the CRS-TLE group is not apparent, and thus further study is required. It is however worth noting that the thalamus holds a relatively large population of GABAergic neurons, and that absence seizures are generated within the thalamocortical loop (60). Additionally, Cope et al. (65) demonstrated that an increased GABAergic inhibition may cause absence seizures through an impaired uptake of GABA through its transporters. The difference in levels of this metabolite between the two groups may therefore be an indicator of the separate roles GABA has in the regulation of temporal lobe and absence seizures. Furthermore, as this study only

encompasses the thalamic metabolism, it cannot be excluded that there may be more metabolic differences in other brain areas.

5.5. Limitations of this study

Although a lot of information was obtained from this study, there are still several limitations to it that should be pointed out. One of these is the fact that the TLE group only contained four rats (originally six, but two died as a consequence of the SE). This made it very difficult to obtain statistical significance, as the variations within the group often were large. Thus, a larger number of rats should be included in future studies.

Furthermore, there are several drawbacks with the lithium-pilocarpine rat model, especially with regards to the extent of damage caused by SE. This is often more extensive than what is seen in human patients, and thus the model may not reproduce the human condition as well as initially believed (112). In any case, as TLE is such a heterogeneous disorder, it is clear that any model will only be representative of a subgroup of patients.

Another limitation of this study worth mentioning is the fact that the NMR and HPLC techniques give no information about the whereabouts of the metabolites. Some indication on where synthesis is taking place is given by ^{13}C-NMRS; however, this is still limited. Furthermore, it cannot give information about whether the metabolite is intra- or extracellularly, to mention one example. Since cells are highly compartmentalised, a lot more valuable information could potentially be obtained if knowledge about this was available. Moreover, this study only gives a snapshot of the metabolism at a specific time point. Thus, a longitudinal study using *in vivo* MRS would be interesting in order to detect changes over time.

6. Conclusion

In this study, ^{1}H-NMRS, ^{13}C-NMRS and HPLC were used to address several research questions, with the first one being what effects chronic TLE had on the interictal thalamic metabolism in adult rats. Here it was found that both the glucose consumption as well as the TCA cycle activity were reduced, which may either indicate metabolic impairment or cell death. This altered metabolism was in particular the case for the neurons, as the overall glutamine metabolism was relatively unchanged. These results are thus in agreement with several previous studies.

It was then of interest to see whether CRS had an effect on the metabolism in the thalamus of the rats that had been injected with lithium-chloride and pilocarpine. In this case the glucose consumption and NAA levels were similar to those in the control rats, thus indicating that CRS is capable of reducing neuronal cell death and/or restoring mitochondrial metabolism. In spite of this, CRS did not have an effect on the conversion of [1,2-^{13}C]acetate-labelled glutamine into glutamate and GABA, which remained at the same reduced level as for the TLE rats without the CRS treatment.

Finally, the thalamic metabolism was compared between the CRS-treated rats which developed TLE and absence-like epilepsy. In this particular study there were not many differences between the two groups; however, this may not be the case in other regions of the brain. Nevertheless, the GABA content was lower in the rats which developed absence-like epilepsy. Although the cause for this is not apparent, the results may reflect the major role GABA plays in the generation of absence seizures within the thalamocortical loop.

7. References

1. Kettenmann H, Verkhratsky A. Neuroglia: the 150 years after. Trends in Neurosciences. 2008;31(12):653–9.

2. Brady ST, Siegel G, Albers, RW, Price DL. Basic Neurochemistry: Principles of Molecular, Cellular and Medical Neurobiology. Academic Press; 2011.

3. Maolood N, Meister B. Protein components of the blood–brain barrier (BBB) in the brainstem area postrema–nucleus tractus solitarius region. Journal of Chemical Neuroanatomy. 2009;37(3):182–95.

4. Lodish H, Berk A, Zipursky SL, Matsudaira P, Baltimore D, Darnell J. Molecular Cell Biology , 4th ed. New York: W. H. Freeman; 2000.

5. Bear MF, Connors BW, Paradiso MA. Neuroscience. Baltimore: Lippincott Williams & Wilkins; 2007.

6. Yang J-L, Sykora P, Wilson III DM, Mattson MP, Bohr VA. The excitatory neurotransmitter glutamate stimulates DNA repair to increase neuronal resiliency. Mechanisms of Ageing and Development. 2011;132(8–9):405–11.

7. Buttermore ED, Thaxton CL, Bhat MA. Organization and maintenance of molecular domains in myelinated axons. Journal of Neuroscience Research. 2013;91(5):603–22.

8. Sofroniew MV, Vinters HV. Astrocytes: biology and pathology. Acta Neuropathologica. 2010;119(1):7–35.

9. Lee A, Pow DV. Astrocytes: Glutamate transport and alternate splicing of transporters. The International Journal of Biochemistry & Cell Biology. 2010;42(12):1901–6.

10. Wang D, Bordey A. The astrocyte odyssey. Progress in Neurobiology. 2008;86(11):342-67.

11. Seifert G, Steinhäuser C. Neuron–astrocyte signaling and epilepsy. Experimental Neurology. 2011;2(44):4-10.

12. Leybaert L. Neurobarrier coupling in the brain: a partner of neurovascular and neurometabolic coupling? Journal of Cerebral Blood Flow and Metabolism. 2005;25(1):2–16.

13. Gordon GRJ, Mulligan SJ, MacVicar BA. Astrocyte control of the cerebrovasculature. Glia. 2007;55(12):1214–21.

14. Attwell D, Laughlin SB. An energy budget for signaling in the grey matter of the brain. Journal of Cerebral Blood Flow & Metabolism. 2001;21(10):1133–45.

15. Muneer PA, Alikunju S, Szlachetka AM, Mercer AJ, Haorah J. Ethanol impairs glucose uptake by human astrocytes and neurons: protective effects of acetyl-L-carnitine. International journal of physiology, pathophysiology and pharmacology. 2011;3(1):48.

16. Dienel GA. Fueling and imaging brain activation. American Society for Neurochemistry. 2012;4(5):267–321.

17. Schousboe A, Sickmann HM, Bak LK, Schousboe I, Jajo FS, Faek SAA, et al. Neuron-glia interactions in glutamatergic neurotransmission: Roles of oxidative and glycolytic adenosine triphosphate as energy source. Journal of Neuroscience Research. 2011;89(12):1926–34.

18. Garrett RH, Grisham CM. Biochemistry. Belmont: Cengage Learning; 2012.

19. Aires CCP, Soveral G, Luís PBM, Brink HJ, de Almeida IT, Duran M, et al. Pyruvate uptake is inhibited by valproic acid and metabolites in mitochondrial membranes. FEBS Letters. 2008;582(23–24):3359–66.

20. Marin-Valencia I, Roe CR, Pascual JM. Pyruvate carboxylase deficiency: Mechanisms, mimics and anaplerosis. Molecular Genetics and Metabolism. 2010;101(1):9–17.

21. Alberts B, Johnson A, Lewis J, Raff M, Roberts K, Walter P. Molecular Biology of the Cell: Reference Edition. Garland Publishing, Incorporated; 2008.

22. Sitkovsky M, Lukashev D. Regulation of immune cells by local-tissue oxygen tension: HIF1α and adenosine receptors. Nature Reviews Immunology. 2005;5(9):712–21.

23. Chuquet J, Quilichini P, Nimchinsky EA, Buzsaki G. Predominant enhancement of elucose uptake in astrocytes versus neurons during activation of the somatosensory cortex. Journal of Neuroscience. 2010;30(45):15298–303.

24. Nehlig A, Coles JA. Cellular pathways of energy metabolism in the brain: Is glucose used by neurons or astrocytes? Glia. 2007;55(12):1238–50.

25. Pellerin L, Magistretti PJ. Glutamate uptake stimulates Na+,K+-ATPase activity in astrocytes via activation of a distinct subunit highly sensitive to Ouabain. Journal of Neurochemistry. 1997;69(5):2132–7.

26. Qu H, Håberg A, Haraldseth O, Unsgård G, Sonnewald U. (13)C MR spectroscopy study of lactate as substrate for rat brain. Developmental Neuroscience. 2000;22(5-6):429–36.

27. Pellerin L, Bouzier-Sore A-K, Aubert A, Serres S, Merle M, Costalat R, et al. Activity-dependent regulation of energy metabolism by astrocytes: An update. Glia. 2007;55(12):1251–62.

28. Shen J. Modeling the glutamate–glutamine neurotransmitter cycle. Frontiers in Neuroenergetics. 2013;5(1):1-13.

29. Chaudhry FA, Reimer RJ, Edwards RH. The glutamine commute take the N line and transfer to the A. Journal of Cell Biology. 2002;157(3):349–55.

30. Dienel GA, Popp D, Drew PD, Ball K, Krisht A, Cruz NF. Preferential labeling of glial and meningial brain tumors with [2-14C]acetate. Journal of Nuclear Medicine. 2001;42(8):1243–50.

31. Wyss MT, Magistretti PJ, Buck A, Weber B. Labeled acetate as a marker of astrocytic metabolism. Journal of Cerebral Blood Flow Metabolism. 2011<31(8):1668–74.

32. Woo N-S, Lu J, England R, McClellan R, Dufour S, Mount DB, et al. Hyperexcitability and epilepsy associated with disruption of the mouse neuronal-specific K–Cl cotransporter gene. Hippocampus. 2002;12(2):258–68.

33. Fisher RS, Boas W van E, Blume W, Elger C, Genton P, Lee P, et al. Epileptic seizures and epilepsy: Definitions proposed by the International League Against Epilepsy (ILAE) and the International Bureau for Epilepsy (IBE). Epilepsia. 2005;46(4):470–2.

34. Engel J. Report of the ILAE Classification Core Group. Epilepsia. 2006;47(9):1558–68.

35. Sander JW, Shorvon SD. Epidemiology of the epilepsies. Journal of Neurology, Neurosurgery and Psychiatry. 1996;61(5):433–43.

36. Engel Jr J. Introduction to temporal lobe epilepsy. Epilepsy Research. 1996;26(1):141–50.

37. Berg AT, Berkovic SF, Brodie MJ, Buchhalter J, Cross JH, van Emde Boas W, et al. Revised terminology and concepts for organization of seizures and epilepsies: Report of the ILAE Commission on Classification and Terminology, 2005-2009. Epilepsia. 2010;51(4):676–85.

38. Berg AT, Scheffer IE. New concepts in classification of the epilepsies: Entering the 21st century. Epilepsia. 2011;52(6):1058–62.

39. Téllez-Zenteno JF, Hernández-Ronquillo L. A review of the epidemiology of temporal lobe epilepsy. Epilepsy Research and Treatment. 2012;2012:1–5.

40. Semah F, Picot MC, Adam C, Broglin D, Arzimanoglou A, Bazin B, et al. Is the underlying cause of epilepsy a major prognostic factor for recurrence? Neurology. 1998;51(5):1256–62.

41. Blair RDG. Temporal lobe epilepsy semiology. Epilepsy Research and Treatment. 2012;2012:1–10.

42. Epilepsy A. Proposal for revised classification of epilepsies and epileptic syndromes. Epilepsia. 1989;30:389–99.

43. O'Dell CM, Das A, Wallace G, Ray SK, Banik NL. Understanding the basic mechanisms underlying seizures in mesial temporal lobe epilepsy and possible therapeutic targets: A review. Journal of Neuroscience Research. 2012;90(5):913–24.

44. Mathern GW, Babb TL, Vickrey BG, Melendez M, Pretorius JK. The clinical-pathogenic mechanisms of hippocampal neuron loss and surgical outcomes in temporal lobe epilepsy. Brain. 1995;118(1):105–18.

45. Engel J. Update on surgical treatment of the epilepsies: Summary of the second International Palm Desert Conference on the Surgical Treatment of the Epilepsies (1992). Neurology. 1993;43(8):1612–1612.

46. Pitkänen A, Sutula TP. Is epilepsy a progressive disorder? Prospects for new therapeutic approaches in temporal-lobe epilepsy. The Lancet Neurology. 2002;1(3):173–81.

47. Scharfman HE, Goodman JH, Sollas AL. Granule-like neurons at the hilar/CA3 border after Status Epilepticus and their synchrony with area CA3 pyramidal cells: Functional implications of seizure-induced neurogenesis. Journal of Neuroscience. 2000;20(16):6144–58.

48. Angeles DK. Proposal for revised clinical and electroencephalographic classification of epileptic seizures. Epilepsia. 1981;22(4):489-501.

49. Panayiotopoulos MJ. Treatment of typical absence seizures and related epileptic syndromes. Paediatric Drugs. 2001;3(5):379–403.

50. Metzger CD, van der Werf YD, Walter M. Functional mapping of thalamic nuclei and their integration into cortico-striatal-thalamo-cortical loops via ultra-high resolution imaging—from animal anatomy to in vivo imaging in humans. Frontiers in Neuroscience. 2013;7:24.

51. Conn PM. Neuroscience in medicine. Springer; 2008.

52. Arcelli P, Frassoni C, Regondi M, Biasi SD, Spreafico R. GABAergic neurons in mammalian thalamus: A marker of thalamic complexity? Brain Research Bulletin. 1997;42(1):27–37.

53. Mc Alonan K, Brown VJ. The thalamic reticular nucleus: More than a sensory nucleus? The Neuroscientist. 2002;8(4):302–5.

54. Guillery RW, Sherman SM. Thalamic relay functions and their role in corticocortical communication: Generalizations from the visual system. Neuron. 2002;33(2):163–75.

55. Alexander GE, DeLong MR, Strick PL. Parallel organization of functionally segregated circuits linking basal ganglia and cortex. Annual Review of Neuroscience. 1986;9(1):357–81.

56. Seidenberg M, Hermann B, Pulsipher D, Morton J, Parrish J, Geary E, et al. Thalamic atrophy and cognition in unilateral temporal lobe epilepsy. Journal of the International Neuropsychological Society : JINS. 2008;14(3):384–93.

57. Dreifuss S, Vingerhoets F, Lazeyras F, Gonzales Andino S, Spinelli L, Delavelle J, et al. Volumetric measurements of subcortical nuclei in patients with temporal lobe epilepsy. Neurology: Journal of the American Heart Association. 2001;57(9):1636–41.

58. Tuchscherer V, Seidenberg M, Pulsipher D, Lancaster M, Guidotti L, Hermann B. Extrahippocampal integrity in temporal lobe epilepsy and cognition: Thalamus and executive functioning. Epilepsy & Behavior. 2010;17(4):478–82.

59. Bertram EH, Mangan PS, Zhang D, Scott CA, Williamson JM. The midline thalamus: Alterations and a potential role in limbic epilepsy. Epilepsia. 2001;42(8):967–78.

60. Avoli M, Gloor P. Interaction of cortex and thalamus in spike and wave discharges of feline generalized penicillin epilepsy. Experimental neurology. 1982;76(1):196–217.

61. Bertram EH. Temporal lobe epilepsy: Where do the seizures really begin? Epilepsy & Behavior. 2009;14(1, Supplement 1):32–7.

62. Sohal VS, Keist R, Rudolph U, Huguenard JR. Dynamic GABAA receptor subtype-specific modulation of the synchrony and duration of thalamic oscillations. Journal of Neuroscience. 2003;23(9):3649–57.

63. Petroff OAC. Book Review: GABA and glutamate in the human nrain. Neuroscientist. 2002;8(6):562–73.

64. Sirven JI, Noe K, Hoerth M, Drazkowski J. Antiepileptic drugs 2012: Recent advances and trends. Mayo Clinic Proceedings. 2012;87(9):879–89.

65. Cope DW, Di Giovanni G, Fyson SJ, Orban G, Errington AC, Lorincz ML, et al. Enhanced tonic GABAA inhibition in typical absence epilepsy. Nature Medicine. 2009;15(12):1392–8.

66. Henry TR, Mazziotta JC, Engel J Jr. Interictal metabolic anatomy of mesial temporal lobe epilepsy. Archives of Neurology. 1993;50(6):582–9.

67. Spanaki MV KL. Postoperative changes in cerebral metabolism in temporal lobe epilepsy. Archives of Neurology. 2000;57(10):1447–52.

68. Najm IM, Wang Y, Hong SC, Luders HO, Ng TC, Comair YG. Temporal changes in proton MRS metabolites after kainic acid-induced seizures in rat brain. Epilepsia. 1997;38(1):87–94.

69. Dufour F, Koning E, Nehlig A. Basal levels of metabolic activity are elevated in Genetic Absence Epilepsy Rats from Strasbourg (GAERS): measurement of regional activity of cytochrome oxidase and lactate dehydrogenase by histochemistry. Experimental Neurology. 2003;182(2):346–52.

70. Nehlig A, Vergnes M, Marescaux C, Boyet S. Cerebral energy metabolism in rats with genetic absence epilepsy is not correlated with the pharmacological increase or suppression of spike-wave discharges. Brain Research. 1993;618(1):1–8.

71. Löscher W, Schmidt D. New horizons in the development of antiepileptic drugs. Epilepsy Research. 2002;50(1–2):3–16.

72. Loscher W. Animal models of epilepsy for the development of antiepileptogenic and disease-modifying drugs. A comparison of the pharmacology of kindling and post-status epilepticus models of temporal lobe epilepsy. Epilepsy research. 2002;50(1):105–24.

73. Sharma AK, Reams RY, Jordan WH, Miller MA, Thacker HL, Snyder PW. Mesial temporal lobe epilepsy: Pathogenesis, induced rodent models and lesions. Toxicologic Pathology. 2007;35(7):984–99.

74. Curia G, Longo D, Biagini G, Jones RSG, Avoli M. The pilocarpine model of temporal lobe epilepsy. Journal of Neuroscience Methods. 2008;172(2):143–57.

75. Smolders I, Khan GM, Manil J, Ebinger G, Michotte Y. NMDA receptor-mediated pilocarpine-induced seizures: characterization in freely moving rats by microdialysis. British Journal of Pharmacology. 1997;121(6):1171–9.

76. François J, Germe K, Ferrandon A, Koning E, Nehlig A. Carisbamate has powerful disease-modifying effects in the lithium-pilocarpine model of temporal lobe epilepsy. Neuropharmacology. 2011;61(1-2):313–28.

77. Glien M, Brandt C, Potschka H, Voigt H, Ebert U, Löscher W. Repeated low-dose treatment of rats with pilocarpine: low mortality but high proportion of rats developing epilepsy. Epilepsy research. 2001;46(2):111–9.

78. Jope RS, Morrisett RA, Snead OC. Characterization of lithium potentiation of pilocarpine-induced status epilepticus in rats. Experimental neurology. 1986;91(3):471–80.

79. Giblin KA, Blumenfeld H. Is epilepsy a preventable disorder? New evidence from animal models. The Neuroscientist. 2010;16(3):253–75.

80. Waldbaum S, Liang L-P, Patel M. Persistent impairment of mitochondrial and tissue redox status during lithium-pilocarpine-induced epileptogenesis. Journal of Neurochemistry. 2010;115(5):1172–82.

81. Bialer M, White HS. Key factors in the discovery and development of new antiepileptic drugs. Nature Reviews Drug Discovery. 2010;9(1):68–82.

82. Whalley B, Stephens G, Constanti A. Investigation of the effects of the novel anticonvulsant compound carisbamate (RWJ-333369) on rat piriform cortical neurones in vitro. British Journal of Pharmacology. 2009;156(6):994–1008.

83. Bialer M, Johannessen SI, Levy RH, Perucca E, Tomson T, White HS. Progress report on new antiepileptic drugs: A summary of the Tenth Eilat Conference (EILAT X). Epilepsy Research. 2010;92(2-3):89–124.

84. White HS, Srivastava A, Klein B, Zhao B, Choi YM, Gordon R, et al. The novel investigational neuromodulator RWJ 333369 displays a broad-spectrum anticonvulsant profile in rodent seizure and epilepsy models. Epilepsia. 2006;47(S4):200–1.

85. Grabenstatter H, Dudek F. The use of chronic models in antiepileptic drug discovery: the effect of RWJ-333369 on spontaneous motor seizures in rats with kainate-induced epilepsy. Epilepsia. 2004;45(57):197.

86. François J, Boehrer A, Nehlig A. Effects of Carisbamate (RWJ-333369) in two models of genetically determined generalized epilepsy, the GAERS and the Audiogenic Wistar AS. Epilepsia. 2008;49(3):393–9.

87. Faught E, Holmes GL, Rosenfeld WE, Novak G, Neto W, Greenspan A, et al. Randomized, controlled, dose-ranging trial of carisbamate for partial-onset seizures. Neurology. 2008;71(20):1586–93.

88. Lindsay S. High Performance Liquid Chromatography. John Wiley & Sons; 1992.

89. Papadoyannis IN. HPLC in clinical chemistry. Marcel Dekker, Inc.; 1990.

90. McMaster M. HPLC: A practical user's guide. John Wiley & Sons; 2007.

91. Greibrokk T, Lundanes E, Rasmussen K. Kromatografi. 3rd ed. Universitetsforlaget AS; 1998.

92. Dong MW. Modern HPLC for practicing scientists. John Wiley & Sons; 2006.

93. Scopes R. Protein purification: principles and practice. 3rd ed. New York: Springer-Verlag; 1994.

94. Khopkar SM. Basic concepts of analytical chemistry. New Age International; 1998.

95. Keeler J. Understanding NMR Spectroscopy. John Wiley & Sons; 2011.

96. Buxton RB. An Introduction to functional magnetic resonance imaging: Principles and techniques. Cambridge University Press; 2002.

97. Field LD, Sternhell S, Kalman JR. Organic structures from spectra. John Wiley & Sons; 2012.

98. Pavia DL, Lampman, Gary M., Kriz, George, S., Vyvyan, James R. Introduction to spectroscopy. Cengage Learning; 2009.

99. Warren NG. Excel HSC physics. Pascal Press; 2005.

100. Hendrick RE. Breast magnetic resonance imaging. Springer; 2008.

101. Shulman RG, Rothman DL. Brain energetics and neuronal activity: Applications to fMRI and medicine. John Wiley & Sons; 2005.

102. Cerdan S, Künnecke B, Seelig J. Cerebral metabolism of [1, 2-13C2] acetate as detected by in vivo and in vitro 13C NMR. Journal of Biological Chemistry. 1990;265(22):12916–26.

103. Balcli M. Basic 1H- and 13C-NMR spectroscopy. Amsterdam; Boston: Elsevier; 2005.

104. Aureli T, Di Cocco ME, Calvani M, Conti F. The entry of [1-13C]glucose into biochemical pathways reveals a complex compartmentation and metabolite trafficking between glia and neurons: a study by 13C-NMR spectroscopy. Brain Research. 1997;765(2):218–27.

105. Khan N, Leonhard Leenders K, Hajek M, Maguire P, Missimer J, Gregor Wieser H. Thalamic glucose metabolism in temporal lobe epilepsy measured with 18F-FDG positron emission tomography (PET). Epilepsy Research. 1997;28(3):233–43.

106. Dubé C, Boyet S, Marescaux C, Nehlig A. Relationship between neuronal loss and interictal glucose metabolism during the chronic phase of the lithium-pilocarpine model of epilepsy in the immature and adult rat. Experimental Neurology. 2001;167(2):227–41.

107. Melø TM, Nehlig A, Sonnewald U. Metabolism is normal in astrocytes in chronically epileptic rats: a 13C NMR study of neuronal–glial interactions in a model of temporal lobe epilepsy. Journal of Cerebral Blood Flow & Metabolism. 2005;25(10):1254–64.

108. Garzillo CL, Mello LE. Characterization of reactive astrocytes in the chronic phase of the pilocarpine model of epilepsy. Epilepsia. 2002;43(s5):107–9.

109. Eid T, Thomas M, Spencer D, Rundén-Pran E, Lai J, Malthankar G, et al. Loss of glutamine synthetase in the human epileptogenic hippocampus: possible mechanism for raised extracellular glutamate in mesial temporal lobe epilepsy. The Lancet. 2004;363(9402):28–37.

110. Hassel B, Bachelard H, Jones P, Fonnum F, Sonnewald U. Trafficking of amino acids between neurons and glia in vivo. Effects of inhibition of glial metabolism by fluoroacetate. Journal of Cerebral Blood Flow Metabolism. 1997;17(11):1230–8.

111. Storm-Mathisen J, Leknes AK, Bore AT, Vaaland JL, Edminson P, Haug FM, et al. First visualization of glutamate and GABA in neurones by immunocytochemistry. Nature. 1983;301(5900):517–20.

112. Navarro Mora G, Bramanti P, Osculati F, Chakir A, Nicolato E, Marzola P, et al. Does pilocarpine-induced epilepsy in adult rats require status epilepticus? PLoS ONE. 2009;4(6):e5759.

From the diagrams:
http://www.explorecuriocity.org/Portals/2/article%20images/neuron.jpg
http://learn.genetics.utah.edu/content/addiction/reward/cells.html
http://cnx.org/content/m45438/latest/?collection=col11487/latest
http://cwx.prenhall.com/bookbind/pubbooks/morris5/medialib/images/F02_09.jpg

8. Appendix

The tissue extraction

Method	Methanol-chloroform double extraction
Written by	Based on method from Lindy Rae
Original	
Revisions	Mussie Ghezu/ Lars Evje/Ursula Sonnewald
Date	04.09.2012

MOST STEPS HAVE TO BE DONE IN THE FUME HOOD, AND USE NITRILE GLOVES
USE ONLY TUBES MADE OF POLYPROPYLENE AND NOT E.G. POLYSTYRENE

This protocol is revised to consider for the way samples were sent from Strasburg (France).

Chemicals

List of chemicals used in the experiment

Name	**Supplier**	**Catalog number**	**CAS no.**	**Where**
Chloroform ($CHCl_3$)	Sigma	319988	67-66-3	Giftskap nederst
Methanol (CH_3OH)	Lab-Scan	C17C11X	67-56-1	K13
L-2-Aminobutyric acid (α-ABA, $C_4H_9NO_2$)	Fluka	07200	1492-24-6	B36
Water has to be destilled or purified				

Equipment

- Eppendorf Centrifuge 5702R (Germany)
- Elga UltraAnalytic water purification system (Great Britain)
- Grant QBT4 block heater (Great Britain)
- Mettler Toledo XP-205 balance (USA)
- Sonics VCX750 with **stepped** microtip 250 µL – 10 mL (catalog no. 630-0422) ultrasonic processor (USA)

Extraction procedure
The procedure is for up to 150 mg tissue. a-ABA is an internal standard for HPLC
Turn on the centrifuge and set the temperature at 4 °C

1. Make sure you have prepared three sets of test tubes for each sample and label them appropriately. A 5 ml tube (tube 1), another 5 ml tube (tube 2) and a 15 ml tube (tube 3)
2. Use a small spatula with flat ends to scrape brain tissue from eppendorf tube (they were delivered in 0.6 ml eppendorf tubes) into Tube 1
3. Add 300 µL methanol (2 times the tissue weight in mg) into the eppendorf tube. Cut off the tip of the microtip used to transfer the methanol into the eppendorf and use it to scrape any remaining tissue in the tube and mix the tissue in the methanol.

4. Transfer the mixture in the eppendorf tube into Tube 1 using the cut off microtip.
5. Add about 50 µL methanol to the eppendorf tube to rinse any remaining tissue
6. Using the cut off microtip scrape any remaining tissue in the eppendorf tube, mix it well and transfer it to Tube 1.
7. **Add 200 µL[1] 250 µM a-ABA to Tube 1**
8. Sonicate the samples on ice – program 9 (Time 0:00:10; Puls On 01; Puls Off 04; Amplitude 30 %)
9. Look at the sample. If necessary repeat step 4 after waiting approximately 1 minute.
10. Flush the probe with 150 µL water into **tube 1**

NB: For steps 1 to 10 one sample is taken at a time while the other samples are kept in the -80.

11. **All work with chloroform in fume hood:** Add 200 µL chloroform (1.5 times the tissue weight in mg) to each tube.
12. Vortex each tube until you get a milky appearance
13. Centrifuge at 4 °C at 4400 rpm (≈3000 g) for 15 minutes
14. Use a pipette to transfer the top layer (methanol/water phase) to a new tube (**tube 2, use 5 mL tubes for 150 mg tissue**). Store the tube on ice
15. To **tube 1** add 400 µL methanol (3 times the tissue weight in mg), add 300 µL water (2 times the tissue weight in mg) and 100 µL chloroform
16. Vortex
17. Repeat steps 13 and 14
18. To **tube 1** add 200 µL methanol (1.5 times the tissue weight in mg) and 150 µL water (1 times the tissue weight in mg) and vortex.
19. Repeat step 13 and 14
20. Add 200 µL chloroform and 1500 µL water to **tube 2 (see comment below)**
21. Vortex
22. Centrifuge at 4 °C at 4400 rpm for 15 minutes and transfer the top layer to new 15 mL tube **(tube 3)**
23. Add 500 µL water and 100 µL methanol to **tube 2**
24. Repeat step 21 and 22
25. Once frozen (-80 °C) evaporate the methanol/water from **tube 3** using the lyophilizer. **Tube 3** is used for e.g. NMR, GC-MS and HPLC and can be stored at -20 °C.
26. If you need to know the protein concentration use **tube 1** which is left in a fume hood to evaporate the chloroform. Then dissolve the pellet in NaOH and perform protein determination or store in freezer for other analyses.

Tube 2 and the pipette tips used after step 6 must be left in a fume hood to evaporate the chloroform – throw next day.

Comment:
The metanol:water phase in tube 2 will contain lipids. The addition of water in step 16 is done in order to remove the lipids. However, the amount of water in the previous version (protocol from 20120219) is probably not sufficient to remove all the lipids. Therefore the volume of water in step 16 has been increased from 500 µL to 1500 µL.

[1] The amount of a-ABA depends on the volume used to dissolve the sample after lyophilization in step 18. The final concentration of a-ABA in the HPLC sample should be 25 µM